TECHNICAL REPORT

97-28

A mathematical model of past, present and future shore level displacement in Fennoscandia

Tore Påsse

Sveriges geologiska undersökning
Göteborg, Sweden

December 1997

SVENSK KÄRNBRÄNSLEHANTERING AB
SWEDISH NUCLEAR FUEL AND WASTE MANAGEMENT CO

P.O.BOX 5864 S-102 40 STOCKHOLM SWEDEN
PHONE +46 8 665 28 00
FAX +46 8 661 57 19

A MATHEMATICAL MODEL OF PAST, PRESENT AND FUTURE SHORE LEVEL DISPLACEMENT IN FENNOSCANDIA

Tore Påsse

Sveriges geologiska undersökning, Göteborg, Sweden

December 1997

Information on SKB technical reports from1977-1978 (TR 121), 1979 (TR 79-28), 1980 (TR 80-26), 1981 (TR 81-17), 1982 (TR 82-28), 1983 (TR 83-77), 1984 (TR 85-01), 1985 (TR 85-20), 1986 (TR 86-31), 1987 (TR 87-33), 1988 (TR 88-32), 1989 (TR 89-40), 1990 (TR 90-46), 1991 (TR 91-64), 1992 (TR 92-46), 1993 (TR 93-34), 1994 (TR 94-33), 1995 (TR 95-37) and 1996 (TR 96-25) is available through SKB.

A mathematical model of past, present and future shore level displacement in Fennoscandia

Tore Påsse

Sveriges geologiska undersökning
Göteborg, Sweden

December 1997

Keywords: Shore level displacement, glacio-isostatic uplift, eustasy, crustal thickness.

ABSTRACT

Shore level displacement in Fennoscandia is mainly due to two interactive vertical movements, glacio-isostatic uplift and eustatic sea level rise. A recent investigation of the lake-tilting phenomenon (Påsse 1996a) has made it possible to discern the course of glacio-isostatic. As a consequence an iteration process for estimate glacio-isostatic uplift and eustatic rise using empirical data of the shore level displacement has been started.

The model indicates that there are two mechanisms involved in glacio-isostatic uplift, one slow and the other fast. The main uplift, still in progress, acts slowly. A*rctan* functions have proved to be suitable tools for describing slow glacio-isostatic uplift. The time of maximal uplift rate is isochronous, meaning that slow uplift occurred simultaneously in all Fennoscandia in an interactive movement. For slow uplift there is a relationship between the rate of decline and the crustal thickness. In areas with greater crustal thickness the rate of decline of the glacio-isostatic recovery is lower than in areas with thinner crust. The fast mechanism gave rise to a crustal subsidence which started about 12 500 BP. After about 10 300 BP, in the early Holocene, the subsidence was restored by a fast uplift. Normal distribution functions have been used for calculating the fast mechanism.

The mantle material exhibits plastic behaviour. When the mantle encounters short-lived stresses the material behaves like an elastic solid but in response to long-term stresses it will flow. The slow mechanism can be linked to viscous flow and as a response to long-term stresses. The fast mechanism is probably the response to a short-lived stress. This stress could have been caused by renewed ice loading, due to a self-triggered redistribution of the ice load during deglaciation.

Future development regarding glacio-isostatic uplift, eustasy and shore level displacement is predicted in Fennoscandia using the results from the modelling. Predictions are based on the assumption that crustal and eustatic developments will follow trends that exist today.

Development of the Baltic have been outlined in this paper.

SAMMANFATTNING

Strandförskjutningen i området som täcktes av den skandinaviska isen under den senaste istiden utgör en funktion av två samverkande vertikala rörelser, glacial-isostatisk landhöjning och eustatisk havsytehöjning. Ett ungefärligt förlopp av landhöjningen har erhållits genom sjöstjälpningsmetoden (Påsse 1996a). Denna kunskap har gjort det möjligt att matematiskt modellera strandförskjutningsförloppet för att bestämma landhöjningens och havsytans förändringar. Detta har gjorts med utgångspunkt från strandförskjutningsdata samt data över den nuvarande relativa landhöjningen.

Modelleringen har visat att landhöjningen styrs av två mekanismer, en långsam och en snabb rörelse. Rörelsen som styrs av den långsamma mekanismen är pågående och utgör den största delen av den glacial-isostatiska landhöjningen. Den långsamma landhöjningens förlopp har beräknats med hjälp av *arctan*-funktioner. Tidpunkten, då den långsamma landhöjningen var som störst, inföll samtidigt inom hela området vilket visar att rörelsen sker i samverkan. Ett samband har påvisats mellan avklingningshastigheten och jordskorpans tjocklek. I områden med tjock jordskorpa är landhöjningen långsammare än i områden med tunn skorpa. Den snabba mekanismen avspeglas i en landsänkning som började ca 12 500 BP och sedan upphörde ca 10 300 BP. Vid denna tidpunkt ersattes landsänkningen av en snabb landhöjning som pågick under tidig Holocen tid. Den snabba mekanismen har beräknats med hjälp av normalfördelningsfunktioner.

Materialet i manteln visar ett plastiskt beteende. När manteln utsätts för kortvariga tryck reagerar materialet som en elastisk kropp, medan de flyter om de utsätts för långvarig påverkan. Den långsamma mekanismen kan kopplas till viskös massförflyttning och som ett svar på långvarig påverkan. Den snabba mekanismen är troligen ett svar på en kortvarig spänning. Denna kortvariga spänning har troligen orsakats av förnyad islast, som hypotetiskt tillkommit genom en självskapad omfördelning av ismassorna under isavsmältningen.

Den framtida utvecklingen avseende landhöjning, havsyteförändringar och strandförskjutning i Fennoskandia kan förutsägas genom modellen. Dessa förutsägelser bygger på antagandet att jordskorpans rörelser och havsytans förändringar följer de trender som existerar idag.

Östersjöns utveckling har skisserats i arbetet.

TABLE OF CONTENTS

SUMMARY

The objective of the modelling is to find mathematical expressions which describe shore-level displacement in the area covered by the Scandinavian ice during the Weichselian glaciation. The intention is to predict future shore level development and to increase knowledge about the mechanisms of glacio-isostatic uplift.

A mathematical model of shore level displacement in Fennoscandia was recently presented by the author in a SKB Technical Report (Påsse 1996b). One of the results presented in this model was that the rate of decline of glacio-isostatic recovery is related to crustal thickness. The aim of the present paper is to make further analysis of this relationship and to introduce the result in a revised model. The present paper can be regarded as a second edition of the publication from 1996b.

Shore level displacement (S m) in Fennoscandia is mainly due to two interactive vertical movements, glacio-isostatic uplift (U m) and eustatic sea level rise (E m) and is estimated by $S = U - E$. It have been difficult to model shore level displacement due to the lack of empirical data concerning the glacio-isostatic uplift and also the lack of reliable data on eustatic rise. However, according to an investigation of the lake-tilting phenomenon (Påsse 1996a) the course of glacio-isostatic uplift has been discerned. As a consequence an iteration process for estimate glacio-isostatic uplift and eustatic rise using empirical data of the shore level displacement has been started. Shore level displacement is known from 67 shore level curves in the area affected by Scandinavian ice during the Late Weichselian.

The model indicates that there are two mechanisms involved in glacio-isostatic uplift, one slow and the other fast. The main uplift is a slow declining movement. This movement is still in progress in the whole area covered by ice during the Late Weichselian. The peripheral parts of this area, which today seem to be submerged, are thus still affected by a slow uplift. The reason for the submergence is ongoing eustatic rise. The present annual eustatic rise is estimated to be 1.2 mm/y. A*rctan* functions have proved to be suitable tools for describing the slow glacio-isostatic uplift. The slow uplift (U_s m) can be expressed as

$$U_s = 0.6366 \times A_s\,(arctan\,(T_s\,/\,B_s) - \,arctan\,((\,T_s - t\,)\,/\,B_s))$$

where A_s is half of the total uplift (m), T_s (years) is the time for the maximal uplift rate, t (year) is the variable time and B_s is a declining factor. The time for maximal uplift is estimated to be 12 500 calendar years *i.e.* 11 300 conventional radiocarbon years BP. This is a constant value meaning that slow uplift occurred simultaneously in all Fennoscandia in an interactive movement. It also implies that a great part of the uplift, especially in the last deglaciated areas, occurred before the areas were finally ice free. For slow

uplift there is a relationship between the rate of decline and the crustal thickness. In areas with greater crustal thickness the glacio-isostatic recovery is slower than in areas with a thinner crust. The following expression has been established for the relationship between the declining factor and the crustal thickness:

$$B_s = 302\ e^{\ 0.067\ *\ ct}$$

where *ct* is the crustal thickness in km.

The fast mechanism gave rise to crustal subsidence which started about 12 500 BP. After about 10 300 BP, in the early Holocene, the subsidence was restored by a fast uplift. Subsidence is apparent in shore level curves in a peripheral zone outside the Younger Dryas ice margin. Fast uplift is apparent in the same area but also in central Fennoscandia *i.e.* the areas which were rapidly deglaciated during Preboreal time. The fast mechanism has been calculated by normal distribution functions:

$$U_f = A_f \times e^{\ (-0.5\ (((t - Tf)/Bf) \times (t - Tf)/Bf)))}$$

where U_f is the crustal change (m), A_f is the total subsidence/uplift (m), B_f is a declining factor (y^{-1}), t is the variable time (year) and T_f is the time for maximal subsidence and the start of fast uplift, *i.e.* the middle of the function. The modelling indicates a uniform time for this event about 11 500 cal years BP (10 300 y BP).

A formula for expressing eustatic rise is also presented in this paper. The main course of eustatic rise may be expressed as:

$$E = 0.6366 \text{ x } 50 \text{ x } (\arctan\ (9\ 350/1375) - \arctan\ ((9\ 350 - t)/1375))$$

The mantle material exhibits plastic behaviour. When the mantle encounters short-lived stresses the material behaves like an elastic solid but in response to long-term stresses it will flow. The slow mechanism can be linked to viscous flow and as a response to long-term stresses. The fast mechanism is probably the response to a short-lived stress. A great part of the slow uplift, especially in central Fennoscandia, occurred before this area finally became free of ice. Because uplift occurred at different velocities below the ice sheet, recovery in some areas was "delayed". This delay changed the topographical condition below the ice sheet, and is assumed to have caused "glacial-tilting", analogous to the lake-tilting phenomenon. This process is supposed to have triggered redistribution of the ice load during deglaciation which caused an isostatic subsidence, which in turn further amplified the process. The low deglaciation rate during the climatic deterioration at about 11 000 BP amplified the process by a more prolonged period of isostatic delay.

The positions of maximal uplift for slow uplift and fast uplift respectively are situated in different places. This condition supports the assumption that the causes for the slow and fast mechanisms are different. The two mechanisms gave rise to tilting in different directions.

Future development regarding glacio-isostatic uplift, eustasy and shore level displacement can be predicted in Fennoscandia using the results from the modelling. Some shore level curves from sites in Sweden are shown as examples of these predictions, Figure 5-2. The predictions are based on the assumption that crustal and eustatic movements follow trends that exist today.

Shore level curves from the coasts around the Baltic are affected by raised water levels during two lake stages, the Baltic Ice Lake and the Ancylus Lake. Development of the Baltic has been outlined in chapter 6 and is summarised in Figure 6-5.

1 METHOD OF THE MODELLING

1.1 OBJECTIVE

The objective of the modelling is to find mathematical expressions which describe shore-level displacement in the area covered by Scandinavian ice during the Weichselian glaciation. This model is to help predict future shore level development and to increase knowledge about the mechanisms of glacio-isostatic uplift.

A mathematical model of shore level displacement in Fennoscandia was recently presented by the author in a SKB Technical Report (Påsse 1996b). One of the results of the modelling was that the rate of decline of glacio-isostatic recovery is obviously related to crustal thickness. The aim of the present paper is to make further analysis of this relationship and to introduce the result in a revised model. The present paper can be regarded as a second shorter edition of the publication from 1996. Some text has been duplicated in order to make the presentation readable.

1.2 METHOD

Shore level displacement (S m) in Fennoscandia is mainly due to two interactive vertical movements, glacio-isostatic uplift (U m) and global eustatic sea level rise (E m), Figure 1-1. Shore level displacement is estimated by

$$S = U - E \qquad \text{1-1}$$

If the eustatic rise of the sea level rise was known it would be possible to calculate the glacio-isostatic uplift, as empirical data exist for S, by access to shore-level curves. Fairbanks (1989) has published a eustatic curve which is generally accepted and commonly used in shore-level modelling. As will be demonstrated later (Chapter 2.4) the reliability of this curve is insufficient and therfore cannot be used for accurate shore-level calculations.

Physical models of glacio-isostatic recovery have been presented during the last years *e.g.* by McConnel (1968), Cathles (1975), Peltier (1976, 1988, 1991), Clark *et al.* (1978), Nakada & Lambeck (1987, 1989), Fjeldskaar & Cathles (1991), Lambeck (1991) and Nakiboglu & Lambeck (1991). The formulas for the course of glacio-isostatic uplift, used in these models, are derived according to rheological parameters. However there are quite different opinions regarding the rheological parameters among these authors. Påsse (1996a) has made investigations of glacio-isostatic uplift based on the lake-tilting method. The point with empirical lake-tilting investigations is that the course of glacio-isostatic uplift can be expressed in mathematical terms without using rheological assumptions.

Empirical data on glacio-isostatic uplift received from lake-tilting investigations (Påsse 1996a) provided the starting point for the present modelling. Lake-tilting data show the difference in the course of the crustal uplift between two points, Figure 1-2. By magnifying the function, which describes the lake-tilting, it has been possible to start an iteration process which has given mathematical expression for factors involved both within the isostatic movements and the eustatic rise.

Information concerning present *relative* uplift (mm/y), recorded by precision levellings and tide gauge data (e.g. Ekman 1996), has been used in the modelling. Present *absolute* uplift (mm/y) was estimated in the modelling. These values were used for calculating present eustatic rise by taking the difference between present *absolute* uplift and present *relative* uplift at different sites. The answer should be equal at each site. This is utilised in the iteration process.

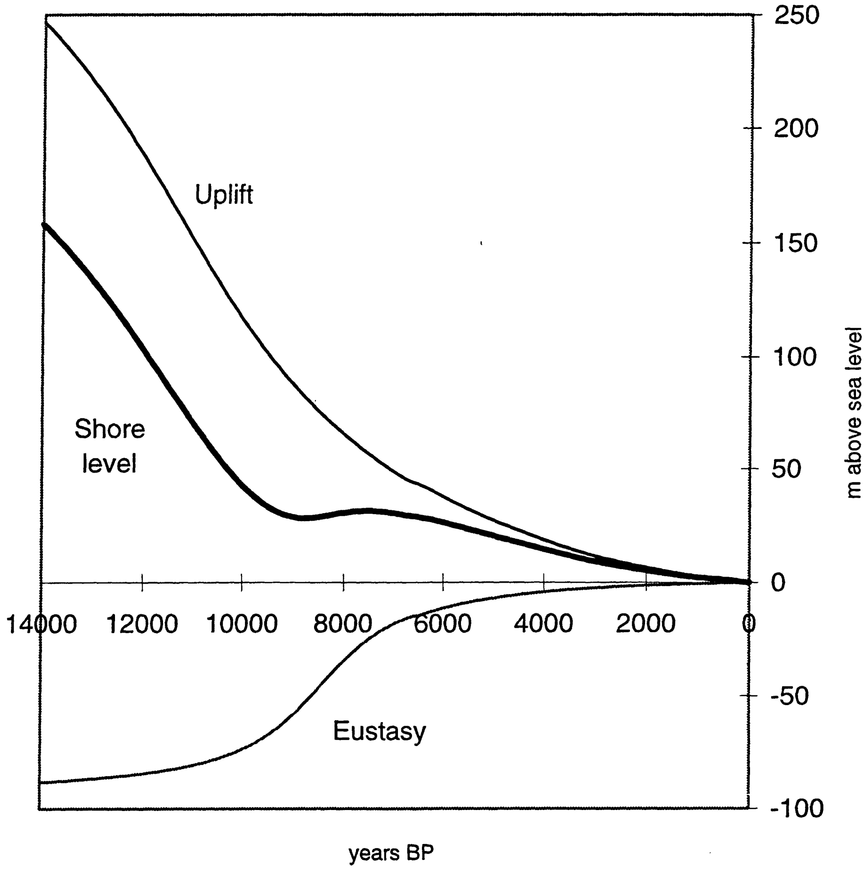

Figure 1-1. *Eustasy (E) and crustal uplift (U) determine shore level displacement (S), by S = U - E.*

Most shore-level curves refer to conventional ^{14}C-dates. However, for calculating the glacio-isostatic uplift it is necessary to use calendar years. A formula for converting conventional ^{14}C-dates to calendar years (Påsse 1996b) is given in Chapter 2.2.

The main input data in the modelling, besides the lake-tilting information, are shore level curves from the area covered by Scandinavian ice during the Late Weichselian. These curves are compared to calculated curves derived in the model. In the first edition 63 shore level curves were used in the analysis and were each shown with a graph comprising the original curve and the theoretical curve plus original data. In the present edition only a selection of these curves are shown. Four new shore level curves have been added to the material. The curves used in the model are designated with site numbers and the geographical positions of the sites are presented in Figure 3-1. The references of the shore level curves are reported in Table 3-1.

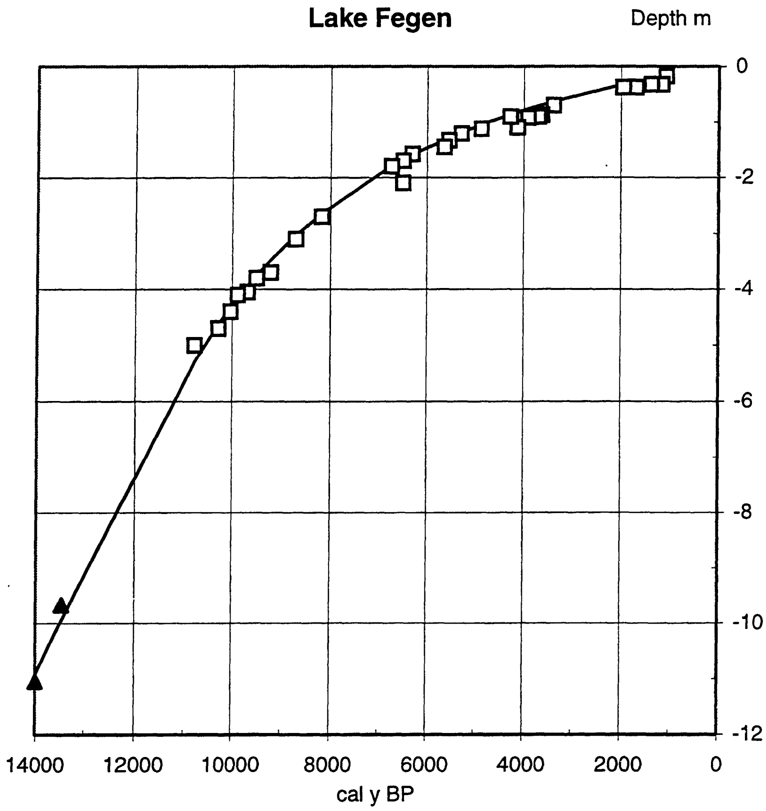

***Figure 1-2**. Radiocarbon dates for ancient lake levels in lake Fegen (Påsse 1990a, 1996a). The two lowermost points, denoted by triangles, are derived from the gradient of shorelines formed during formation of the Göteborg moraine and the Berghem moraine. The curve shows difference in land uplift between the outlet and the southern part of the lake expressed by an arctan function.*

The declining course of the uplift can only be univocal solved using shore level information that extends over a long time span. There are several shore level curves that range just over one or two thousand years. They may be very detailed but due to the short extension of these curves the calculations of uplift would be unreliable using these. Shore level curves comprising long time intervals may be constructed by approximate datings but may in spite of this give better qualifications for uplift calculations than shorter more detailed curves.

It is impossible to present the model in a logical order as every parameter has been determined gradually and dependent of all the other parameters in a multivariable system. What can prove the validity of the model is the congruity between empirical shore level curves and theoretically deduced curves.

2 FORMULAS USED IN THE MODELLING

2.1 GENERAL

Iterative calculations provide a base for the modelling. Access to mathematical expressions which can be used for calculating the development through time are required. This chapter displays the integral parts in the modelling and the formulas used for each part. The formulas are summarised in Chapter 3.3.

2.2 CALIBRATION OF ^{14}C - VALUES

A mathematical expression for converting conventional ^{14}C-dates to calendar dates is derived in Påsse (1996b). The formula used in the modelling for converting dates is written as:

$$t = 59.6 - 206.9 \times arctan\,((4000 - 1.095t_{con})/800) + 63.66 \times arctan\,((7200 - 1.095t_{con})/100)) + 95.5 \times arctan\,((750 - 1.095t_{con})/200) + 1.095t_{con} \qquad 2\text{-}1$$

where t is the calibrated date, while t_{con} is the conventional radiocarbon date. When calendar years are used, this is pointed out by writing cal years BP, while conventional ^{14}C -years are denoted as years BP.

2.3 THE UPLIFT FORMULAS

The first modelling showed that there are two mechanisms involved in glacio-isostatic uplift, one slow and the other fast. The main uplift, still in progress, acts slowly. The fast mechanism gave rise to a crustal subsidence during Alleröd and Younger Dryas restored by fast uplift during early Holocene. The nature of the two mechanisms will be further discussed in Chapter 3.2.

2.3.1 The slow mechanism

According to Andrews (1970) glacio-isostatic movement starts slowly, reaches a maximal rate and after that follows a declining course. Different S-shaped functions have been tested for describing glacio-isostatic uplift from lake-tilting information (Påsse 1996a) and shore level data (Påsse

1996b). *Arctan* functions turned out to be the most suitable way of describing glacio-isostatic uplift following the slow mechanism.

The *arctan* functions can be divided into two symmetrical parts, one is inclining and the other is declining. To say that the initial inclining phase of uplift is symmetrical to the declining phase is an overstatement as there is too little information accessible for testing the inclining phase. The lack of data is due to the fact that the main part of uplift, during the inclining phase, occurred beneath a cover of ice. Only the declining phase of the function can be tested for its validity of describing glacio-isostatic uplift. Land uplift following unloading of ice (U_s in m) can then be described with the function

$$U_s = A_s - (2A_s/\pi) \times arctan\ ((T_s - t)/B_s) - (A_s - (2A_s/\pi) \times arctan\ (T_s / B_s)) \quad 2\text{-}2$$

simplified as

$$U_s = 0.6366 \times A_s\ (arctan\ (T_s / B_s) - arctan\ ((T_s - t) / B_s)) \quad 2\text{-}3$$

where A_s is half of the total uplift (m), T_s (years) is the time for the maximal uplift rate, *i.e.* the middle of the function, t (year) is the variable time and B_s (y^{-1}) is a declining factor. In the calculations T_s and t are counted in calendar years according to formula 2-1. However, within all graphs the dates are reported in conventional ^{14}C- years as these dates are more familiar to most geologists.

The parameters A_s and B_s are related to the position while T_s seems to be regionally constant and is estimated to 12 500 calendar years BP *i.e.* 11 300 years BP counted in the conventional radiocarbon chronology. The formula for the slow uplift can thus be written as

$$U_s = 0.6366 \times A_s\ (arctan\ (12\,500 / B_s) - arctan\ ((12\,500 - t) / B_s)) \quad 2\text{-}4$$

In the southern parts of Scandinavia glacio-isostatic recovery can be calculated using a formula comprising only the slow mechanism. Graphs of two different uplift curves following the slow mechanism are shown in Figure 2-1.

2.3.2 The fast mechanism

Shore level curves from Norway and from the northern parts of the Swedish west coast, *i.e.* areas outside but close to the Younger Dryas ice border, show crustal subsidence during Alleröd and Younger Dryas (about 12 000-10 300 years BP). Shore level curves which prove this subsidence are marked by an asterisk in Table 3-2. After about 10 300 BP, in early Holocene, the subsidence was restored by a fast uplift, lasting about 1000 - 2000 years. The fast uplift during early Holocene is significant in central Fennoscandia and recorded in most shore level curves from this area.

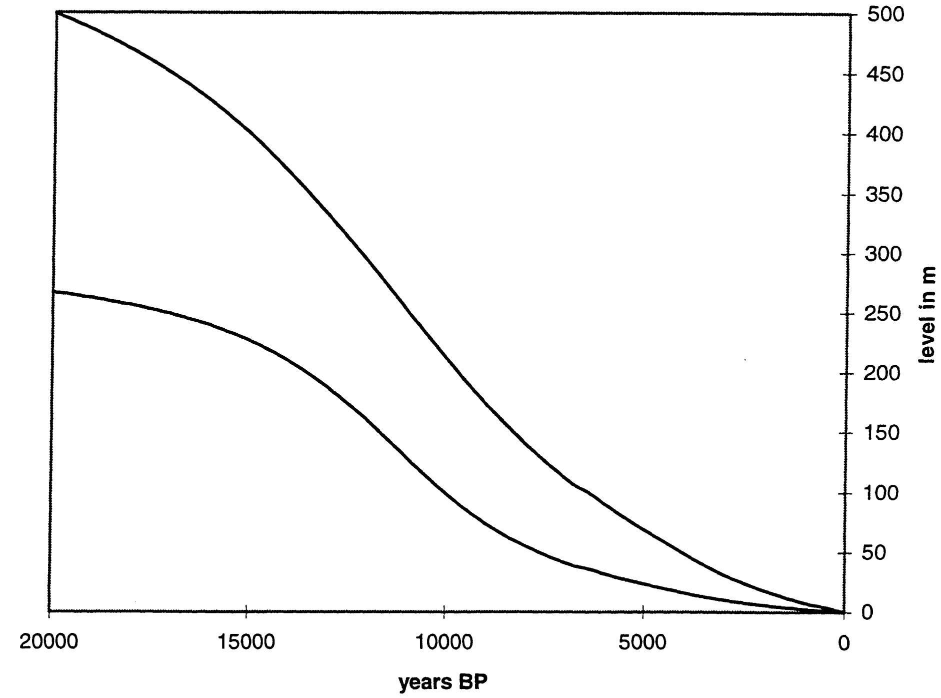

Figure 2-1. *Graphs of slow glacio-isostatic uplift calculated by different values of A_s and B_s. The uppermost curve is calculated with A_s = 380 m and B_s = 6500 and the lowermost curve is calculated with A_s = 170 m and B_s = 3800.*

In the first edition the fast mechanism was described by two reverse *arctan* functions, starting with a negative function for the subsidence followed by a positive function for the recovery. In the present model the fast mechanism is calculated by normal distribution functions. This revision involves a reinterpretation of the course of this mechanism compared to the interpretation discussed in the first edition. For shore level curves from the area outside the Younger Dryas ice border the changes between the two editions are small as the sum of two reverse arctan functions describe a course similar to one normal distribution function. However, for the area inside the Younger Dryas ice border there is a significant difference between the two models regarding the fast mechanism. The calculations of the theoretical shore level curves give quite similar results but there is a fundamental difference in the mechanism. In the first edition it was assumed that subsidence did not affect the area inside the Younger Dryas ice border. This assumption lacks proof as shore level curves from this area do not derive from the actual period. In the present model it is assumed that central Fennoscandia, in the area inside the Younger Dryas ice border, was affected by subsidence in analogy to the condition established outside the ice border.

A general formula for the fast mechanism is:

$$U_f = A_f \times e^{(-0.5\,(((t - Tf)/Bf) \times (t - Tf)/Bf)))} \qquad \text{2-5}$$

where U_f is the crustal change (m), A_f is the total subsidence/uplift (m), B_f is a declining factor (y^{-1}), t is the variable time (year) and T_f is the time for the maximal subsidence and the start of the fast uplift, *i.e.* the middle of the function. The modelling indicates a uniform time for this event about 11 500 cal years BP (10 300 y BP). A general formula for the fast mechanism can then be written as:

$$U_f = A_f \times e^{(-0.5\,(((t - 11\,500)/Bf) \times (t - 11\,500)/Bf)))} \qquad \text{2-6}$$

The course of the crustal movements, caused by the fast mechanisms, are shown graphically in Figures 2-2. The total glacio-isostatic uplift can be calculated by combining the effects of the slow and fast movements, Figure 2-3, according to:

$$U = 0.6366 \times A_s\,(\arctan\,(12\,500 / B_s) - \arctan\,((12\,500 - t) / B_s)) +$$

$$+ A_f \times e^{(-0.5\,(((t - 11\,500)/Bf) \times (t - 11\,500)/Bf)))} \qquad \text{2-7}$$

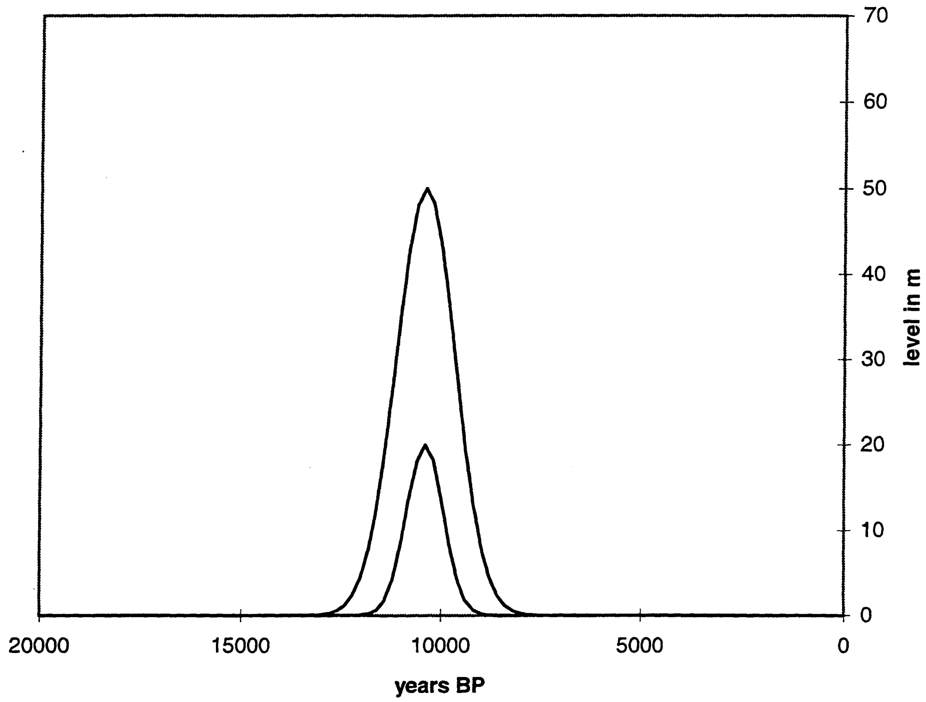

Figure 2-2. *The course of the crustal movements, caused by the fast mechanisms, calculated with A_f = 50 m and B_f = 800 and A_f = 20 m and B_f = 500.*

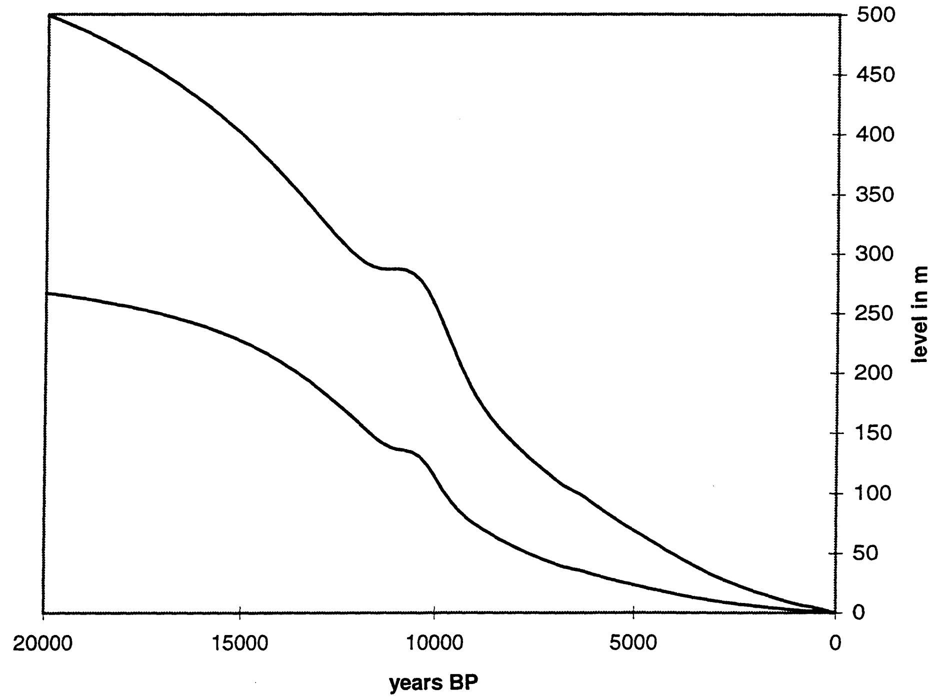

Figure 2-3. Graph of the combination of the crustal movements shown in Figures 2-1 and 2-2.

2.4 THE EUSTASY

The first publication ever of a well-documented shore-level curve is from Göteborg and was made by the Geological Survey of Sweden (Sandegren & Johansson 1931). This curve shows a transgression during the Holocene which was interpreted as land subsidence following the Late Glacial uplift. It was not until Daly (1934) introduced the theory of glacio-eustasy that this transgression was correctly interpreted as a rise of the global sea level. Glacio-eustasy is a climatically controlled movement caused by removal or addition of water under conditions of glaciation and deglaciation.

Ever since Godwin *et al.* (1958), Fairbridge (1961), Jelgersma (1961) and Shepard (1963) presented eustatic curves of the global sea level rise there have been several subsequent curves which on the whole show the same trend but differ in detail. A eustatic curve from Barbados, published by Fairbanks (1989) based on radiocarbon dated corals, is the most generally accepted curve today. This curve goes back to 18 000 years BP and the global sea level was then measured to about - 120 m.

Formula 1-1 can be used to test the validity of eustatic curves. If the empirical data from a shore level curve (S) is added to data from a eustatic curve (E) the course of the crustal movement (U) will be shown. In

Fennoscandia the configuration of such calculated uplift curve should *a priori* be congruent to a magnified empirical estimated lake-tilting curve. This test is done by adding the Fairbanks (1989) eustatic curve to a shore level curve from Sandsjöbacka (Påsse 1987). The uplift curve received by this addition is compared to a magnified empirical estimated lake-tilting curve, based on data from Lake Fegen (Påsse 1996a), Figure 2-4. Lake Fegen is situated close to and at the same isobase as the Sandsjöbacka area in southwestern Sweden. The configuration of the calculated curve does not correspond to magnified lake-tilting curve. The differences between the two curves are shown graphically in Figure 2-5. This graph indicates the size of discrepancy within the Fairbanks (1989) eustatic curve.

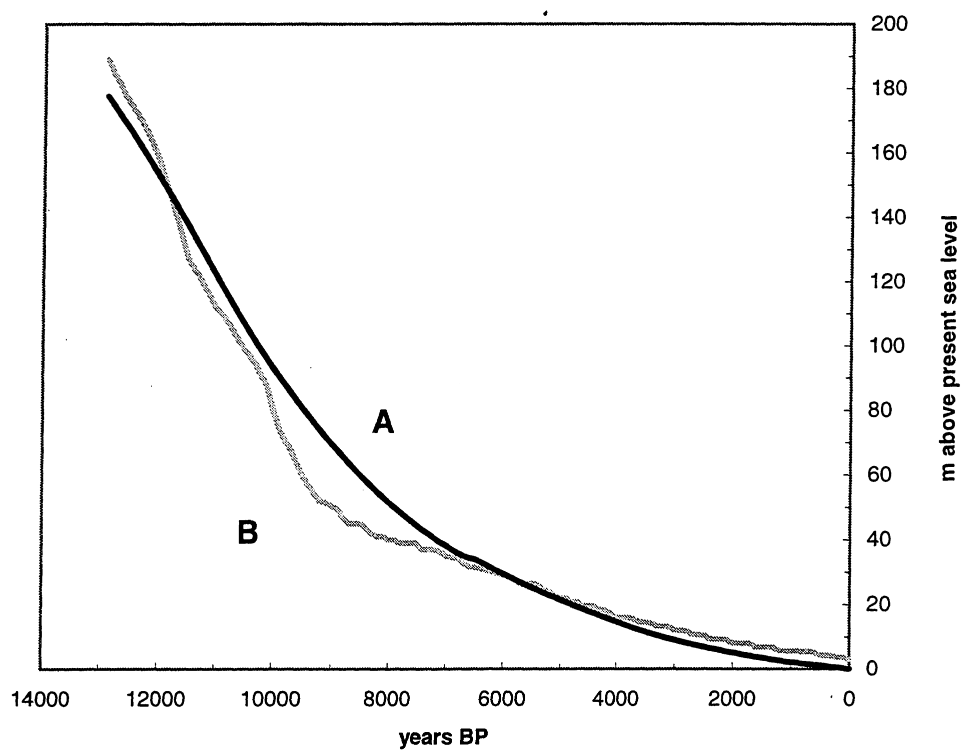

Figure 2-4*. The black curve (A) is a magnified empirical estimated lake-tilting curve, based on data from Lake Fegen (Påsse 1996a). The grey curve is an uplift curve (B) calculated for testing the reliability of Fairbanks (1989) eustatic curve. This uplift curve is derived by addition of the shore level curve (S) from Sandsjöbacka (Påsse 1987) and Fairbanks (1989) eustatic curve (E). In Fennoscandia the configuration of such calculated uplift curve should a priori be congruent to a magnified empirical estimated lake-tilting curve. The differences between the two curves are shown in Figure 2-5.*

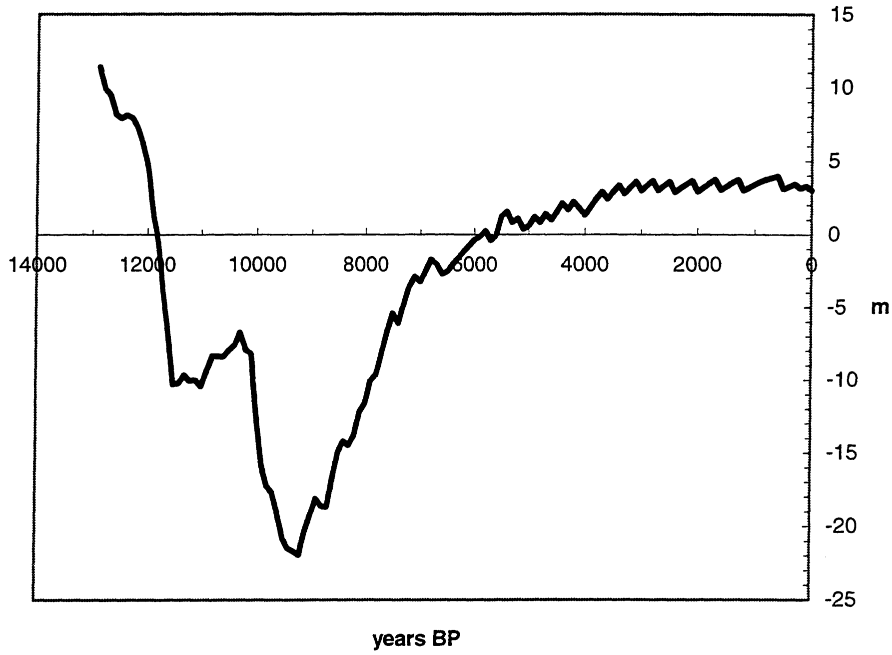

Figure 2-5*. The differences between the two curves shown in Figure 2-4. The graph indicates the size of discrepancy within Fairbanks (1989) eustatic curve.*

A eustatic curve is obtained as a result of the modelling in a similar way to that outlined above. By calculating the difference between hypothetical uplift curves and empirical shore level curves it has been possible, by iteration, to estimate a function for the eustasy. The main course of the eustatic rise may be expressed as:

$$E = 0.6366 \times 50 \times (arctan\,(9\,350/1375) - arctan\,((9\,350 - t)/1375)) \qquad 2\text{-}8$$

This relation is shown in Figure 2-6. Figure 50 in formula 2-8 designates half of the total eustatic rise (in m). This figure shows that, since the glacial maximum, eustatic rise is 100 m according to formula 2-8. However, information concerning the eustasy has only been calculated back to 14 000 y BP in the modelling. *t* in formula 2-8 is in calendar years. The figure 9 350 in this formula means the time for the maximal rate of eustatic rise in calendar years (about 8 450 y BP).

Function 2-8 for the eustasy only takes the main rise into consideration. In areas where the tidal effect is very low and raised shore levels exist, it is obvious that sea level not only rose continuously during Holocene but also changed in an oscillatory way (*cf.* Påsse 1983). The size and periodicity of these oscillations are not satisfactorily known but it is difficult to leave such information unnoticed in this context. A sinusoidal function may be added to the main eustatic formula in order to attain more detailed information regarding transgression and regression phases. The sinusoidal function is preliminary given a periodicity of about 475 years (Påsse 1983) and an amplitude of 0.5 m. The cyclic function can be written as:

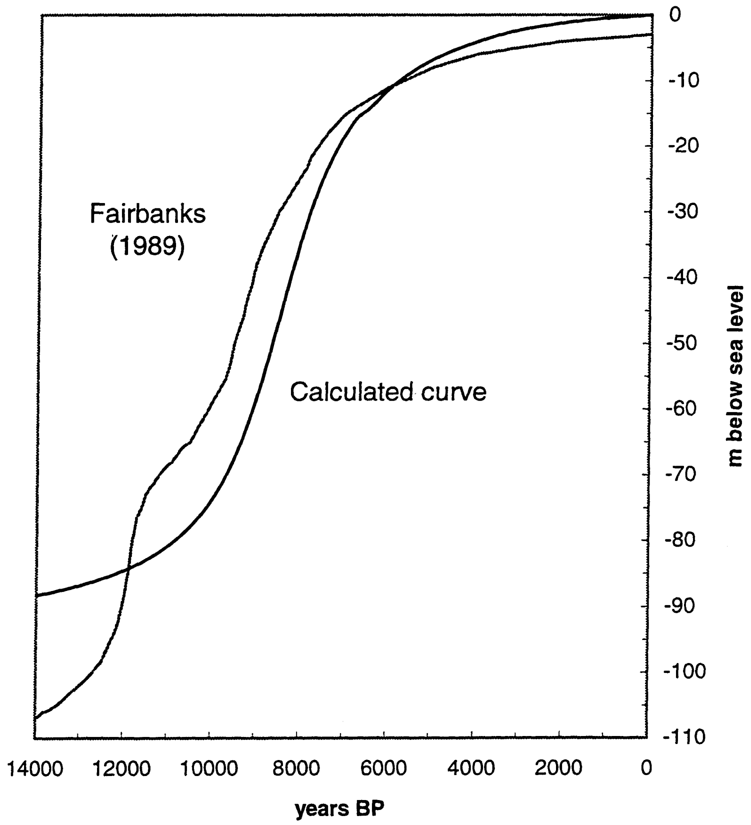

Figure 2-6. *A comparison between Fairbanks (1989) eustatic curve and the curve resulting from the calculations.*

$C = 0.5 \text{ x } sin\ ((t - 100) \text{ x } 0.013)\text{-}0.48$ 2-9

Figure 2-7 shows eustatic changes when function 2-9 is added to 2-8.

Most curves, interpreted as eustatic curves, are derived from off shore information. According to Bloom (1967) sea floor is affected by the change of load caused by the increase of water during eustatic rise. Bloom (1967) named this phenomenon the hydro-isostatic effect. Eustatic curves compiled from submarine information, e.g. Fairbanks curve (1989), ought to be corrected for the hydro-isostatic effect. A eustatic curve, constructed by subtracting the shore level displacement from a "known" glacio-isostatic uplift, does not need this adjustment provided the shore level curve is compiled from an area situated above the present sea level.

The eustatic curve, which is obtained from the modelling, is supposed to illustrate more clearly the trends in global eustasy than *e.g.* the curve presented by Fairbanks (1989). A comparison between Fairbank´s curve and the calculated curve is described in Figure 2-6.

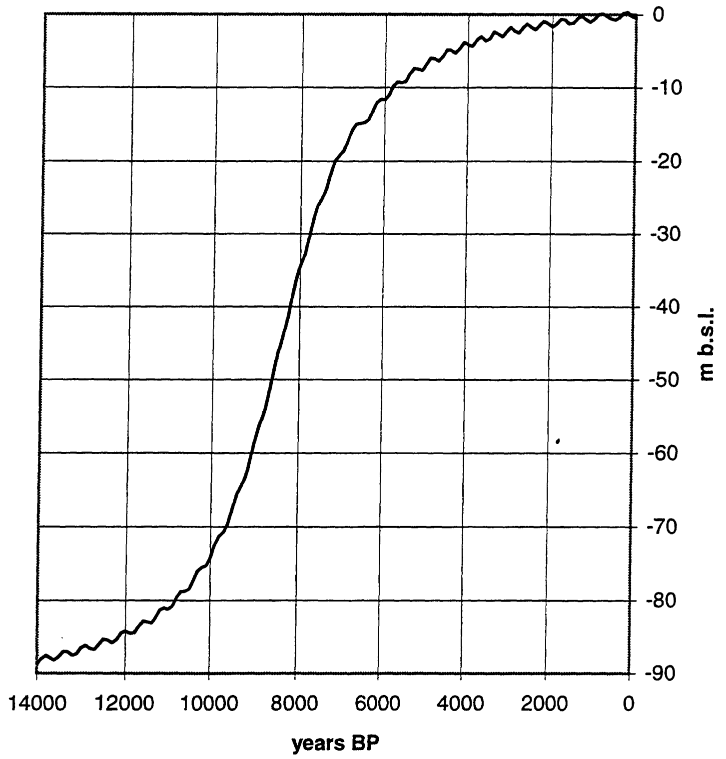

Figure 2-7*. Eustatic rise calculated by a combination of formulas 2-8 and 2-9.*

2.4.1 Water level changes in the Baltic

Shore level curves from the Baltic basin are influenced not only by eustasy but also by water level changes during two lake stages, the Baltic Ice Lake and the Ancylus Lake. The differences between sea level and the lake levels within the Baltic basin were not used in the calcualtions of the shore level curves in the first edition as this information was received as a result of the modelling. In the present second edition theoretically calculated differences between the sea level and the lake levels within the Baltic basin are used in the calculations. These differences are summarised in Figure 6-5.

3 RESULTS OF THE MODELLING

3.1 SHORE LEVEL CURVES

67 shore level curves from the area covered by Scandinavian ice during the Late Weichselian are used as input data in the modelling. These shore level curves are compared to theoretical curves deduced from the formulas presented in Chapter 2. Some examples of these comparisons are shown in Figures 3-2 to 3-7. In these figures original curves are drawn in grey and theoretical curves in black. Original data for constructing the curves are shown by black triangles in the graphs. Each curve used in the analysis is designated with a site number. Geographical positions of the sites are shown in Figure 3-1 and the references are presented in Table 3-1. Sites which are illustrated by shore level curves are marked with an asterisk in Table 3-1. Some shore level curves are complemented or extended by new data from nearby sites. Most of the theoretical curves are calculated without using the oscillation formula, 2-9. The uplift parameters, used for calculating the shore level curves, are reported in Table 3-2.

In the first edition 63 shore level curves were used in the analysis and were each shown graphically in that presentation. Four new shore level curves have been available after the publication of the first edition. These curves are inserted in this second edition and shown in Figure 3-2, 3-3 and 3-7.

Table 3-1. Number, names and references of the sites used in the calculations. Sites which are illustrated by shore level curves are marked with an asterisk.

Nr	Sites	References
1	Varanger	Donner 1980
2	Andöja	Vorren et al. 1988
3	Tromsö	Hald & Vorren 1983
4	Lofoten	Möller 1984, Vorren & Moe 1986
5	Näröy*	Ramfjord 1982
6	Verdalsöra*	Sveian & Olsen 1984
7	Frosta*	Kjemperud 1986
8	Bjugn*	Kjemperud 1986
9	Hitra	Kjemperud 1986
10	Tjeldbergodden*	Solem & Solem 1997
11	Fröja	Kjemperud 1986
12	Leinöy*	Svendsen & Mangerud 1990
13	Fonnes	Kaland 1984
14	Sotra*	Krzywinski & Stabell 1984, Kaland et al 1984
15	Bömlo	Kaland 1984
16	Yrkje	Anundsen 1985

Nr	Sites	References
17	Hardanger*	Helle et al. 1997
18	Jären	Thomsen 1982, Bird & Klemsdal 1986
19	Kragerö*	Stabell 1980
20	Porsgrunn	Stabell 1980
21	Vestfold*	Henningsmoen 1979
22	Oslo	Hafsten 1983
23	Östfold*	Danielsen 1970
24	Ski*	Sörensen 1979
25	Vendsyssel	Rickardt 1996
26	Vedbäck*	Christensen 1993
27	Söborg Sö	Mörner 1976
28	St Bält & Fakse Bugt*	Christensen 1993, Bennike & Jensen 1995
29	Kroppefjäll*	Björck & Digerfeldt 1991
30	Hunneberg	Björck & Digerfeldt 1982
31	Central Bohuslän*	Miller & Robertsson 1988
32	Ljungskile	Persson 1973
33	Risveden*	Svedhage 1985
34	Göteborg	Påsse 1983
35	Sandsjöbacka*	Påsse 1987
36	Fjärås	Påsse 1986
37	Varberg*	Påsse 1990b, Berglund 1995
38	Falkenberg	Påsse 1988
39	Halmstad	Caldenius et al. 1949, Caldenius et al. 1966, Berglund 1995
40	Bjäre*	Mörner 1980b
41	Barsebäck	Digerfeldt 1975, Persson 1962, Ringberg 1989
42	Blekinge*	Björck 1979, Liljegren 1982
43	Oskarshamn*	Svensson 1989
44	Gotland	Svensson 1989
45	Rejmyra*	Persson 1979
46	Stockholm area*	Åse 1970, Miller & Robertsson 1982, Brunnberg et al. 1985, Risberg 1991
47	Eskilstuna	Robertsson 1991
48	Gästrikland	Asklund 1935
49	Hälsingland	G. Lundqvist 1962
50	Ångermanland*	Cato 1992
51	S. Västerbotten	Renberg & Segerström 1981
52	Rovaniemi*	Saarnisto 1981
53	Lauhanwuori*	Salomaa 1982, Salomaa & Matiskainen 1983
54	Satakunta	Eronen 1983
55	Olkiluoto*	Eronen et al 1995
56	Åland*	Glückert 1978
57	Turku	Glückert 1976, Salonen et al. 1984
58	Karjalohka	Glückert & Ristaniemi 1982
59	Tammisaari-Perniö*	Eronen et al 1995
60	Lohja	Glückert & Ristaniemi 1982
61	Espo*	Hyvärinen 1980, 1984, Glückert & Ristaniemi 1982, Eronen & Haila 1982
62	Porvoo*	Eronen 1983
63	Hangassuo	Eronen 1976
64	Tallin	Kessel & Raukas 1979
65	Southern Lithuania*	Kabailienė 1997
66	Western Baltic*	Winn et al 1986, Klug 1980
67	Dalnie Zelentsy*	Snyder et al. 1996

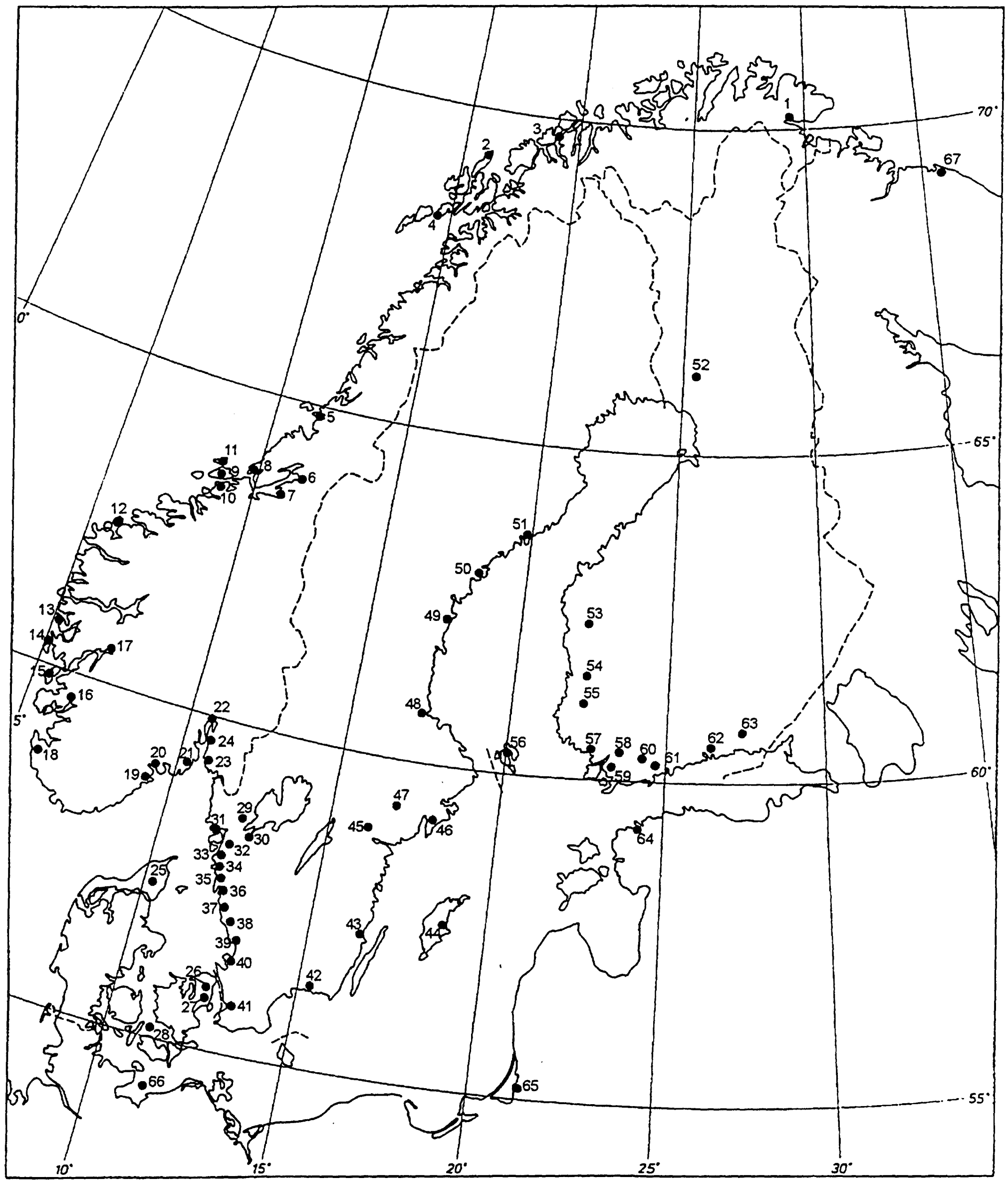

Figure 3-1. ***Position of shore level curves used in the modelling. Numbers refer to Table 3-1, where names of the sites and references are listed.***

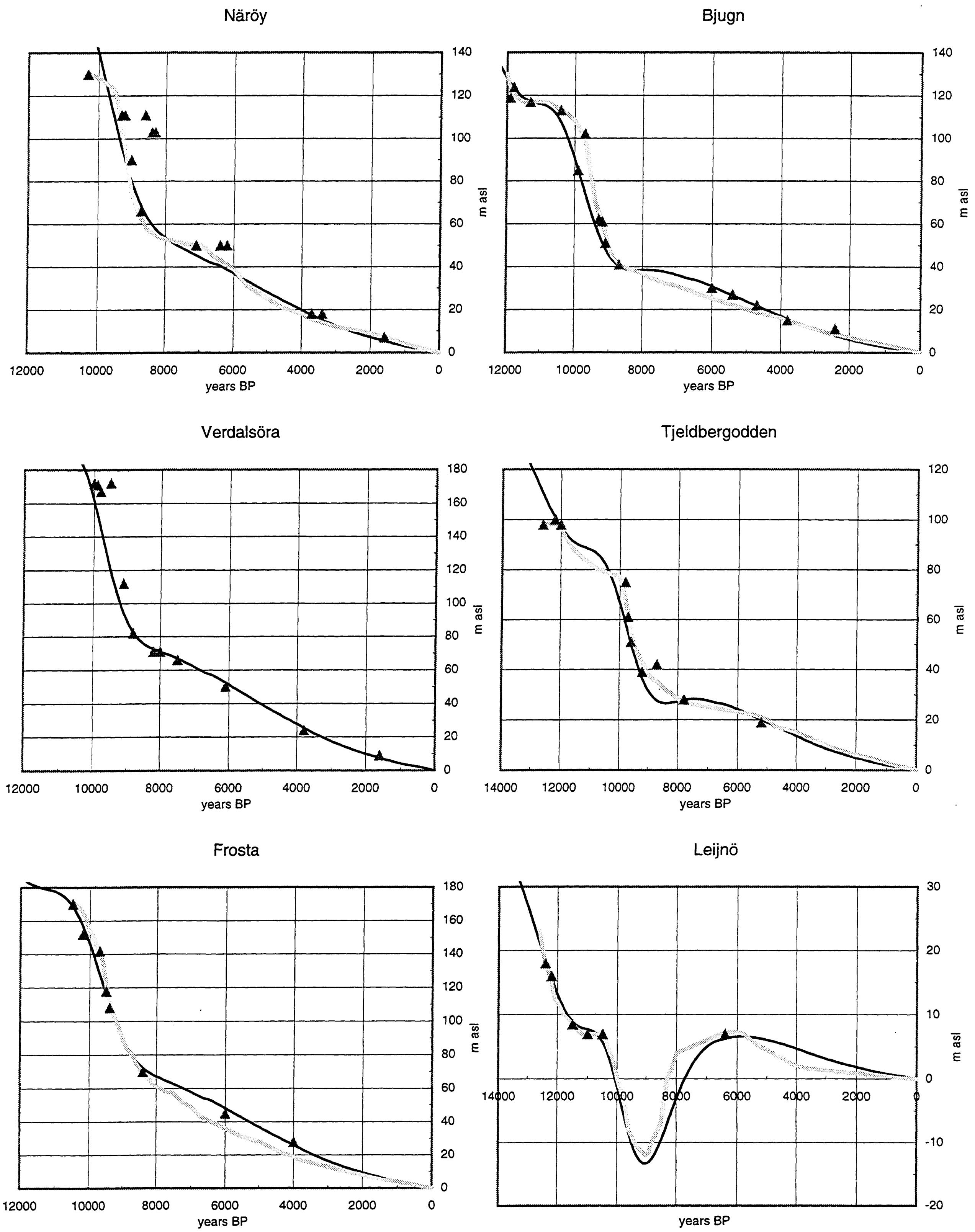

Figure 3-2. *Shore level displacement at Näröy (Ramfjord 1982), Verdalsöra (Sveian & Olsen 1984), Frosta (Kjemperud 1986), Bjugn (Kjemperud 1986), Tjeldbergodden (Solem & Solem 1997) and Leinöy (Svendsen & Mangerud 1990).*

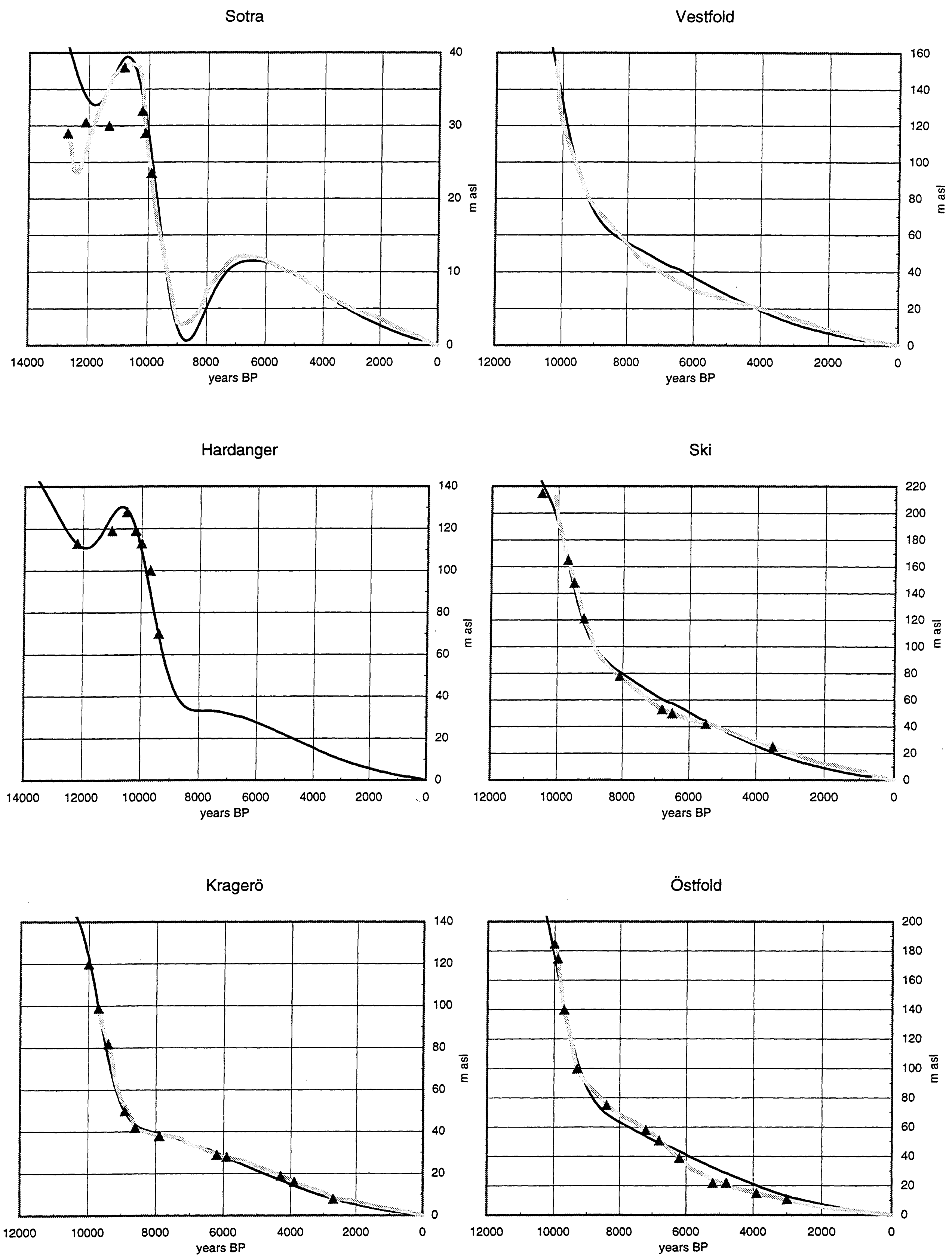

Figure 3-3*. Shore level displacement at Sotra (Krzywinski & Stabell 1984, Kaland et al. 1984), Hardanger (Helle et al. 1997), Kragerö (Stabell 1980), Vestfold (Henningsmoen 1979), Ski (Sörensen 1979) and Östfold (Danielsen 1970).*

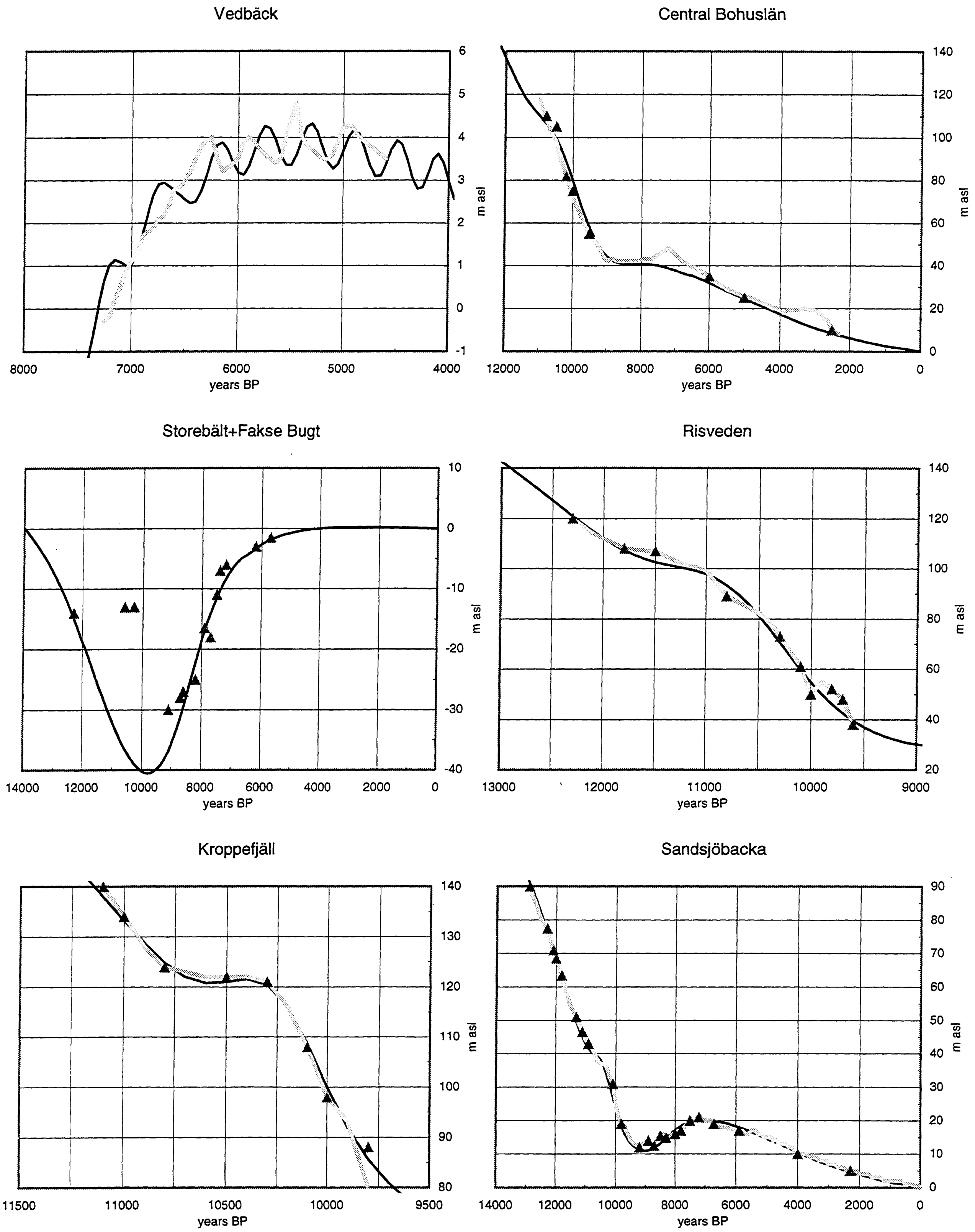

Figure 3-4. Shore level displacement at Vedbäck (Christensen 1993), Storebält + Fakse Bugt (Christensen 1993, Bennike & Jensen 1995), Kroppefjäll (Björck & Digerfeldt 1991), Central Bohuslän (Miller & Robertsson 1988), Risveden (Svedhage 1985) and Sandsjöbacka (Påsse 1983, 1987).

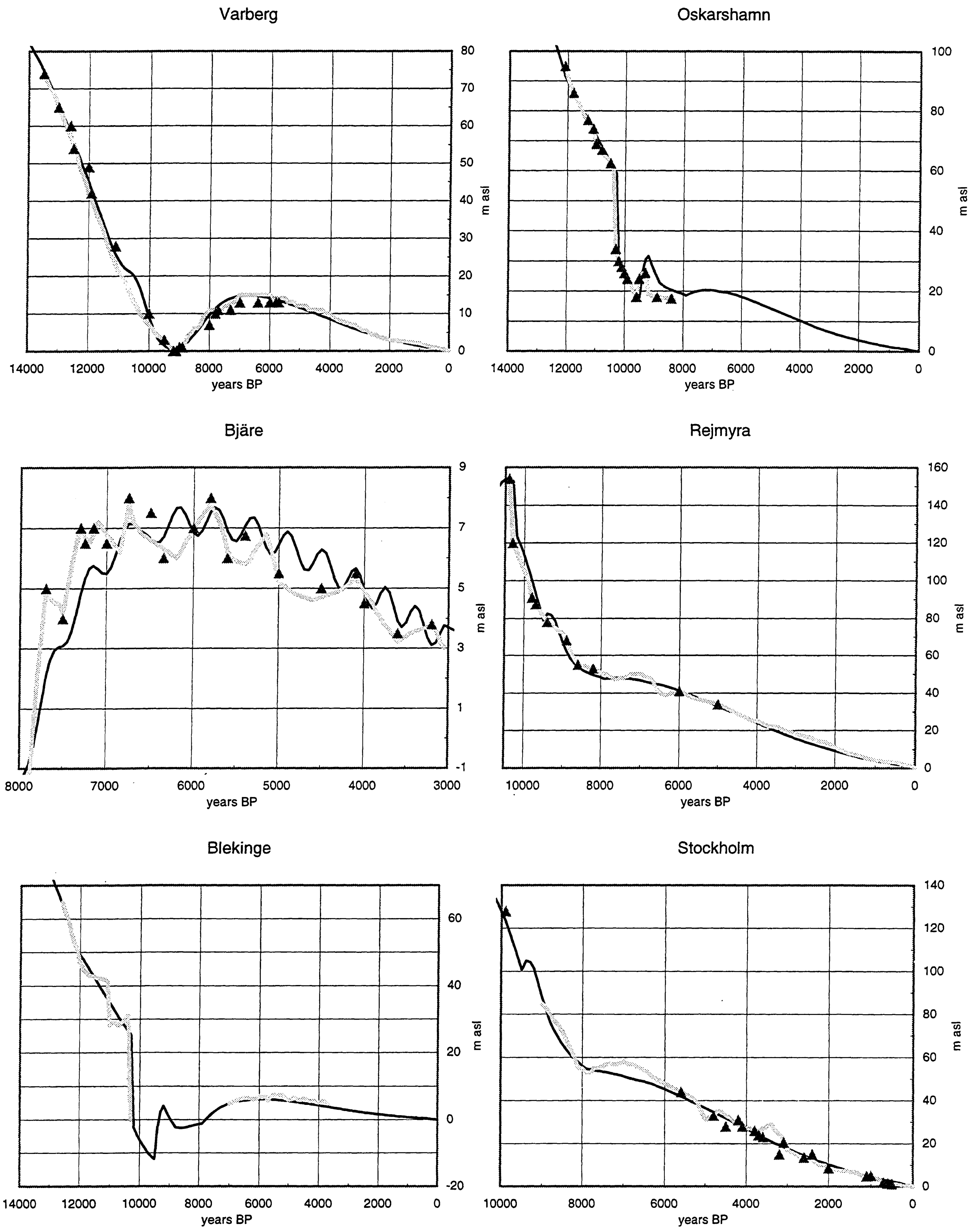

***Figure 3-5**. Shore level displacement at Varberg (Påsse 1983, Berglund 1995), Bjäre (Mörner 1980b), Blekinge (Björck 1979, Liljegren 1982), Oskarshamn (Svensson 1989), Rejmyra (Persson 1979) and Stockholm (Åse 1970, Miller & Robertsson 1982, Brunnberg et al. 1985, Risberg 1991).*

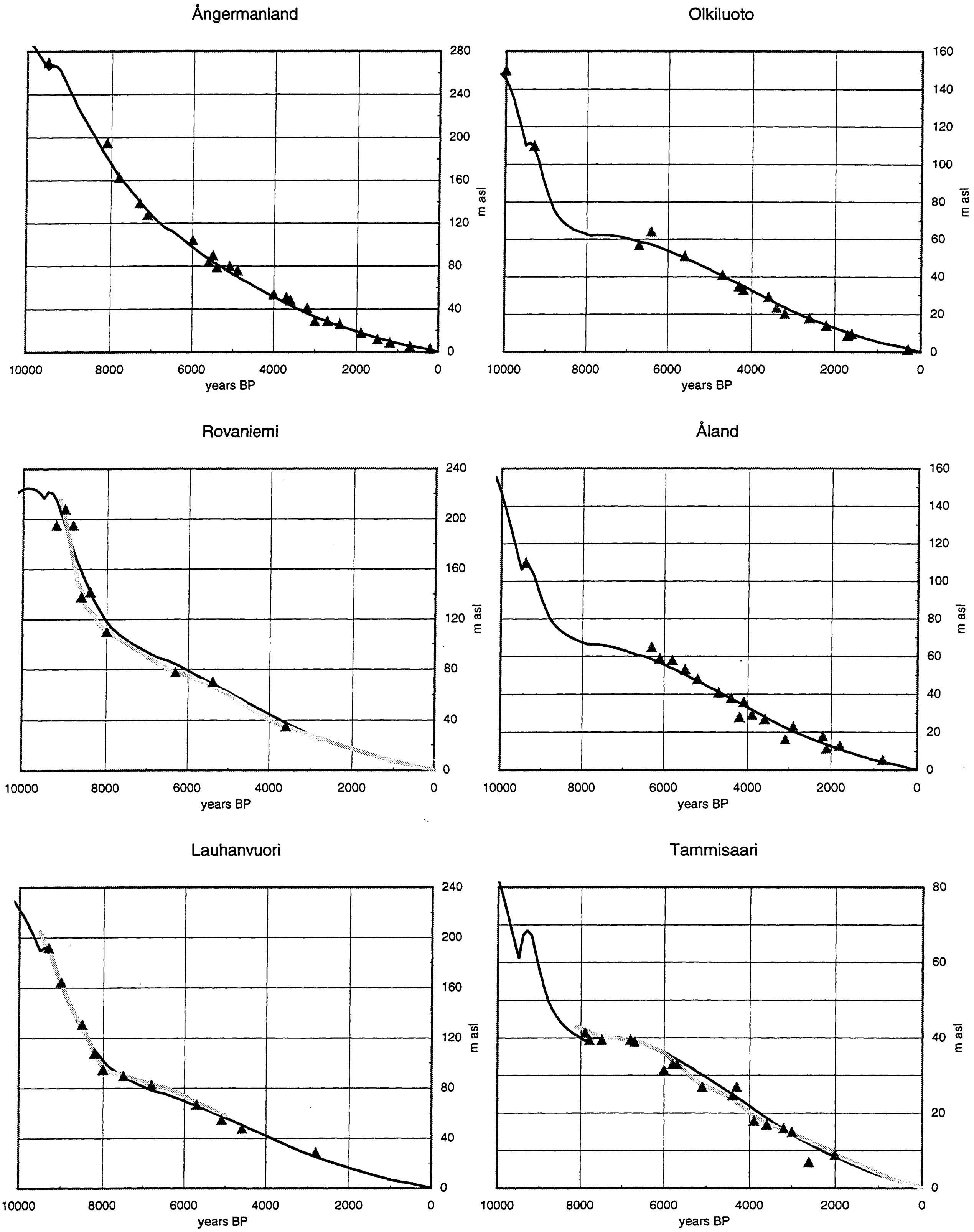

Figure 3-6*. Shore level displacement at Ångermanland (Cato 1992), Rovaniemi (Saarnisto 1981), Lauhanvuori (Salomaa 1982), Olkiluoto (Eronen et al. 1995), Åland (Glückert 1978) and Tammisaari (Eronen et al. 1995).*

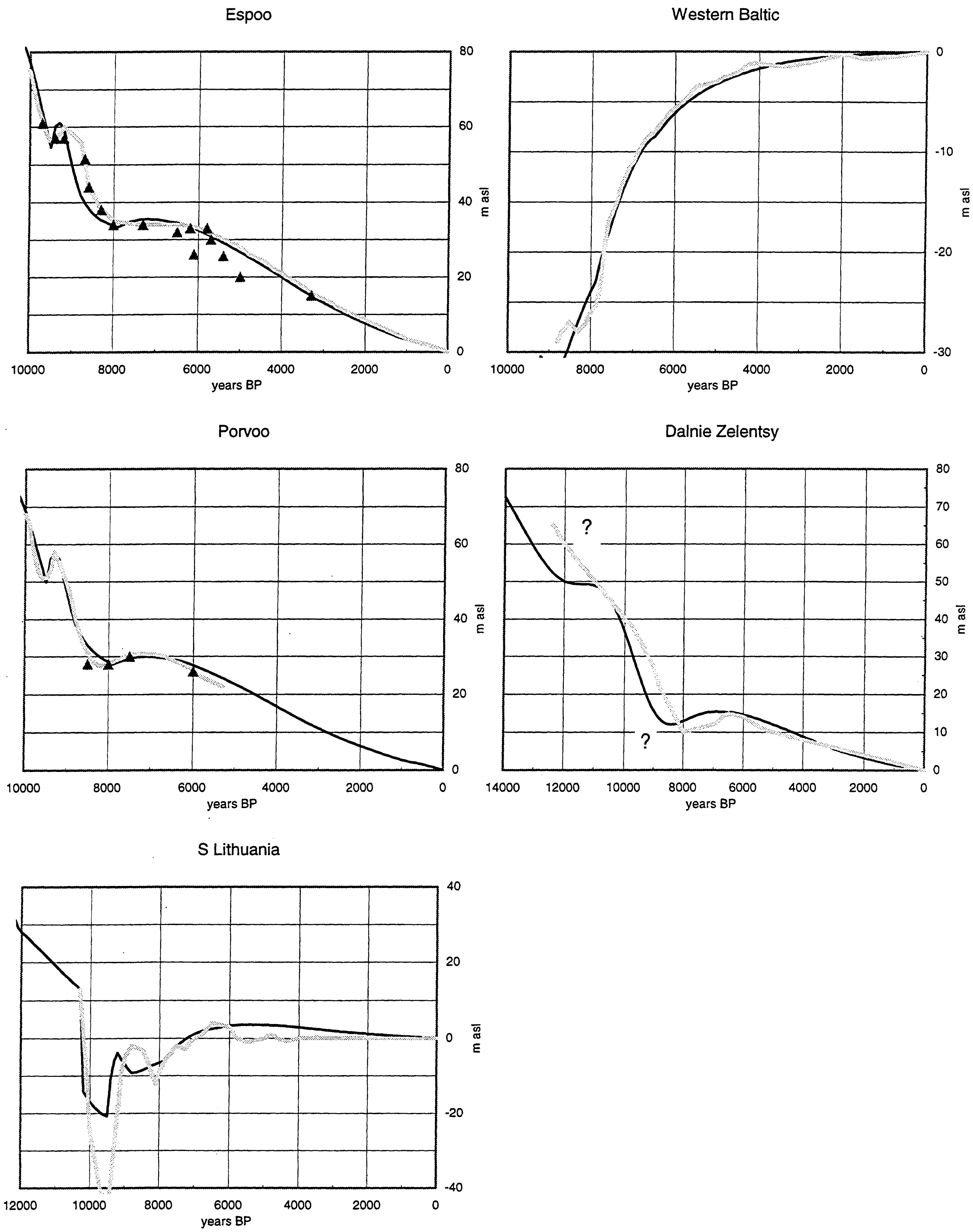

Figure 3-7. *Shore level displacement at Espoo (Hyvärinen 1980, 1984, Glückert & Ristaniemi 1982, Eronen & Haila 1982), Porvoo (Eronen 1983), Southern Lithuania (Kabailiene 1997), Western Baltic (Winn et al. 1986, Klug 1980) and Dalnie Zelentsy (Snyder et al. 1996).*

3.2 GLACIO-ISOSTATIC UPLIFT

3.2.1 General

Lake-tilting investigations (Påsse 1996a) show that slow glacio-isostatic uplift still is in progress with a declining course in the southern parts of Sweden. The shore level modelling shows that slow uplift is in progress in the whole area covered by ice during the Late Weichselian. The peripheral parts of this areas, which today seem to be submerged, are thus still affected by a slow uplift. The reason for the submergence is ongoing eustatic rise.

The uplift parameters used for calculating the theoretical shore level curves, are shown in Table 3-2. The values of A_s, B_s and A_f are also presented in isoline maps, Figures 3-8, 3-11 and 3-13. These maps can be used for determining the specific parameters necessary for calculating shore level displacement at any optional site.

Table 3-2. The uplift parameters used for calculating theoretical shore level curves. Sites, which give information of both subsidence and uplift related to the fast mechanism, are marked with an asterisk.

Site	A_s m	T_s cal year	B_s year^{-1}	A_f m	T_f cal year	B_f year^{-1}
1 Varanger	160	12500	5000	55	11500	1100
2 Andöja	88	12500	3600	20	11500	1200
3 Tromsö*	130	12500	3800	20	11500	800
4 Lofoten	110	12500	3600	20	11500	1000
5 Näröy*	255	12500	3800	60	11500	1000
6 Verdalsöra	305	12500	4400	67	11500	800
7 Frosta*	290	12500	4400	56	11500	1000
8 Bjugn*	223	12500	3800	40	11500	800
9 Hitra*	195	12500	3800	30	11300	600
10 Tjeldbergodden*	188	12500	3800	35	11500	900
11 Fröja*	163	12500	3800	22	11000	650
12 Leinöy*	100	12500	3500	17	11500	800
13 Fonnes	125	12500	3700	30	11500	1000
14 Sotra*	120	12500	3800	37	11500	900
15 Bömlo*	120	12500	3800	30	11500	1000
16 Yrkje*	124	12500	4000	36	11500	800
17 Hardanger*	200	12500	4000	75	11500	900
18 Jären*	95	12500	3400	36	11500	800
19 Kragerö	295	12500	2400	40	11500	900
20 Porsgrunn	325	12500	2400	50	11500	800
21 Vestfold	360	12500	2400	15	11500	700
22 Oslo	435	12500	2700	60	11500	700
23 Östfold	390	12500	2400	50	11500	700
24 Ski	425	12500	2650	45	11500	700
25 Jylland	117	12500	3400	15	11500	600
26 Vedbäck	107	12500	2500			
27 Söborg Sö	98	12500	2500			

Site	A_s m	T_s cal year	B_s year^{-1}	A_f m	T_f cal year	B_f year^{-1}
28 St Bält	62	12500	2500			
29 Kroppefjäll*	282	12500	3700	19	11350	250
30 Hunneberg*	242	12500	4300	29	11900	600
31 C Bohuslän	245	12500	3500	20	11500	400
32 Ljungskile	217	12500	3900	10	11500	350
33 Risveden*	205	12500	3650	25	11900	600
34 Göteborg	170	12500	3700	10	11500	350
35 Sandsjöbacka*	161	12500	3650	9	11500	350
36 Fjärås	155	12500	3700	8	11500	350
37 Varberg	137	12500	3700	7	11500	350
38 Falkenberg	125	12500	3700	6	11500	350
39 Halmstad	118	12500	3300	6	11500	350
40 Bjäre Peninsula	108	12500	3300			
41 Barsebäck	95	12500	2500			
42 Blekinge	125	12500	2500			
43 Oskarshamn	177	12500	3200			
44 Gotland	170	12500	3200			
45 Rejmyra	220	12500	6500	75	11500	800
46 Stockholm area	233	12500	7200	82	11500	1050
47 Eskilstuna	250	12500	7000	90	11500	900
48 Gästrikland	333	12500	7200	95	11500	1000
49 Hälsingland	395	12500	7000	120	11500	1400
50 Ångermanland	430	12500	6500	130	11500	1900
51 S Västerbotten	430	12500	6700	135	11500	1900
52 Rovaniemi	378	12500	6500	115	11500	1100
53 Lauhanwuori	330	12500	9200	140	11500	1300
54 Satakunta	287	12500	9200	110	11500	1200
55 Olkiluoto	265	12500	8600	90	11500	900
56 Åland	285	12500	7000	85	11500	750
57 Turku	235	12500	7500	80	11500	950
58 Karjalohka	215	12500	7500	70	11500	850
59 Tammisaari	195	12500	7200	58	11500	1000
60 Lohja	190	12500	7200	65	11500	900
61 Espo	180	12500	7200	60	11500	900
62 Porvoo	163	12500	6500	57	11500	1000
63 Hangassuo	160	12500	6500	60	11500	900
64 Tallin	165	12500	4500	15	11500	700
65 S Lithuania	105	12500	2500			
66 W Baltic	41	12500	2200			
67 Dalnie Zelentsy	133	12500	4000	35	11500	1200

3.2.2 The slow mechanism

The time for maximal uplift rate (T_s) is estimated to a constant age of 12 500 calendar years *i.e.* 11 300 years BP. T_s is thus isochronous meaning that slow uplift occurred simultaneously in all Fennoscandia in an interactive movement. It also implies that a great part of the uplift, especially in the last deglaciated areas, occurred before the sites finally became free of ice.

The isoline map showing A_S (m) values, which represent half of the total values for slow uplift, is based only on the information received from the 67 shore level curves. Figure 3-8. The configuration of the two highest isolines (450 and 500 m) are drawn as symmetrical extrapolations as data is lacking from this area.

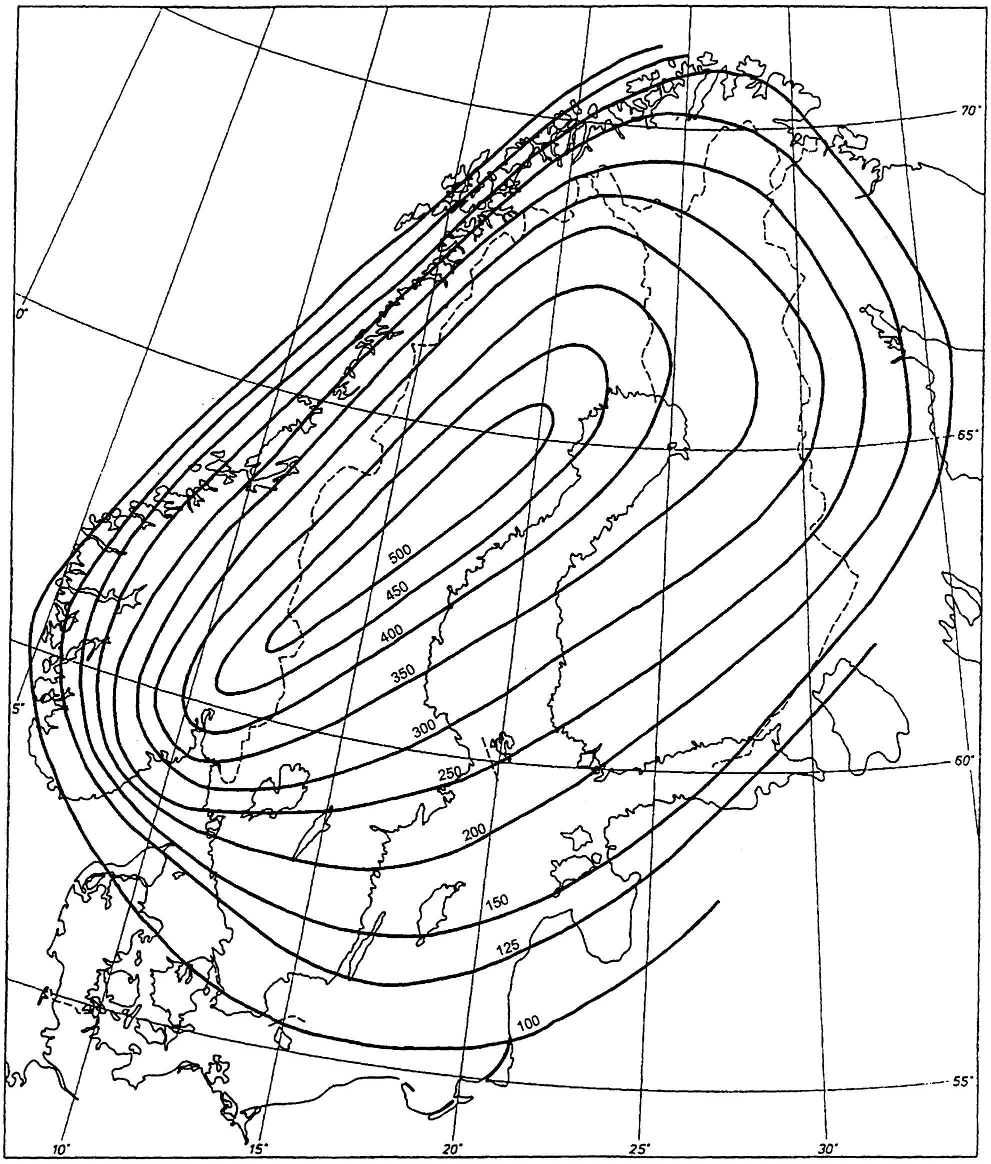

Figure 3-8. *A_S (m) values, i.e. half of the total values for the slow uplift mechanism.*

The configuration of the isolines of present apparent uplift, Figure 4-1 and 4-2, shows a maximum in the Skellefteå area. This maximum is conventionally used for estimating the "centre of the glacio-isostatic uplift" or "the ice divide of the latest glaciation". This interpretation is based on the assumption of a constant declining factor. However, one of the main conclusions, presented in this paper, is that there are regional differences in the rate of the decline. Figure 3-8 infers that "the centre of the glacio-isostatic uplift" and therefore also "the ice divide of the last glaciation" was situated along an axis from Trysil in Norway to Arvidsjaur in northern Sweden.

The accuracy of the estimate of declining factor B_s varies as reliable estimate only can be derived from shore level curves comprising long time periods. The accuracy of determination is estimated to be $\pm$ 10 % for long shore level curves, while the range may be $\pm$ 20 % for the shorter curves. High values of B_s produce flat uplift curves, while low values give steeper curves where most of the recovery occurred close to T_s. The remaining uplift is thus greater in areas with high values of B_s, which also means that the present rise is still relatively fast in these areas. In the first edition of this study the estimate of B_s gave rise to values which were clustered around 6 "mean values". When these values were plotted in a map a relationship between the declining factor and the crustal thickness was discernible. This relationship has been examined and utilised in this second edition.

3.2.3 Crustal thickness

The crustal thickness, the Moho depth, is generally detected by deep seismic sounding. Maps of crustal thickness have been presented by Meissner *et al.* (1987), Ziegler (1990), Giese & Buness (1992) and Kinck *et al.* (1993). The maps from Giese & Buness (1992) and Kinck *et al.* (1993) are shown in Figures 3-9 and 3-10. A comparison between these maps shows that there are relatively large differences in interpretations of crustal thickness. This complicates the aim of this paper of finding a relationship between the declining factor and the crustal thickness. The map from Kinck *et al.* (1993) has been favoured in this investigation, mainly because it embraces all Fennoscandia.

Examination of the relationship between the crustal thickness and the declining factor B_s started by plotting the original values of B_s (Påsse 1996b) versus the crustal depth received from Kinck *et al.* (1993). The values of B_s in the clusters were then either increased or decreased, based on information about crustal depths, if these changes fitted the shore level information. From this revision an exponential expression was established for the relationship between the declining factor and the crustal thickness:

$$B_s = 302\ e^{0.067 * ct} \qquad 3\text{-}1$$

where *ct* is the crustal thickness in km. The isoline map of B_s, shown in Figure 3-11, was drawn by combining the results of the shore level modelling and the configuration of the isolines of the crustal thickness interpreted from seismic soundings by Kinck *et al.* (1993) and Giese & Buness (1992). B_s can thus be determined at any optional site from this map. The values of B_s, corresponding to different crustal thickness, are reported in Table 3-3.

The difference between calculated crustal thickness and geophysical estimate by either Kinck *et al.* (1993) or Giese & Buness (1992) is less than 2 km or corresponds completely for 57 of the 67 sites. The good correspondence for most of the sites indicates the relationship between the declining factor and the crustal thickness. The conformance between the crustal thickness estimated by seismic soundings and "shore level estimate" is shown in Figure 3-12. At ten sites, however, the estimate from the two methods differ considerably. These sites belong to specific areas. In the south-western part of Norway and at Jylland the difference is between 3 and 6 km, and in the Lofoten area, at Oskarshamn - Gotland and at Lithuania the difference is 10 km. There are three possible explanations for the difference in results from the remaining 10 sites: The shore level data are uncertain or misinterpreted; the seismic interpretations are uncertain or misinterpreted; there is yet another factor to consider when determing the rate of decline in some areas. The first explanation is a probable reason for the differences in the Lofoten area, at Jylland and at Lithuania.

Table 3-3. Values of B_s corresponding to different crustal thickness.

Crustal thickness km	B_s	Crustal thickness km	B_s
29	2100	43	5400
30	2200	44	5800
31	2400	45	6200
32	2500	46	6600
33	2700	47	7000
34	3000	48	7500
35	3200	49	8000
36	3400	50	8600
37	3600	51	9200
38	3800	52	9800
39	4100	53	10500
40	4400	54	11200
41	4700	55	12000
42	5000	56	12900

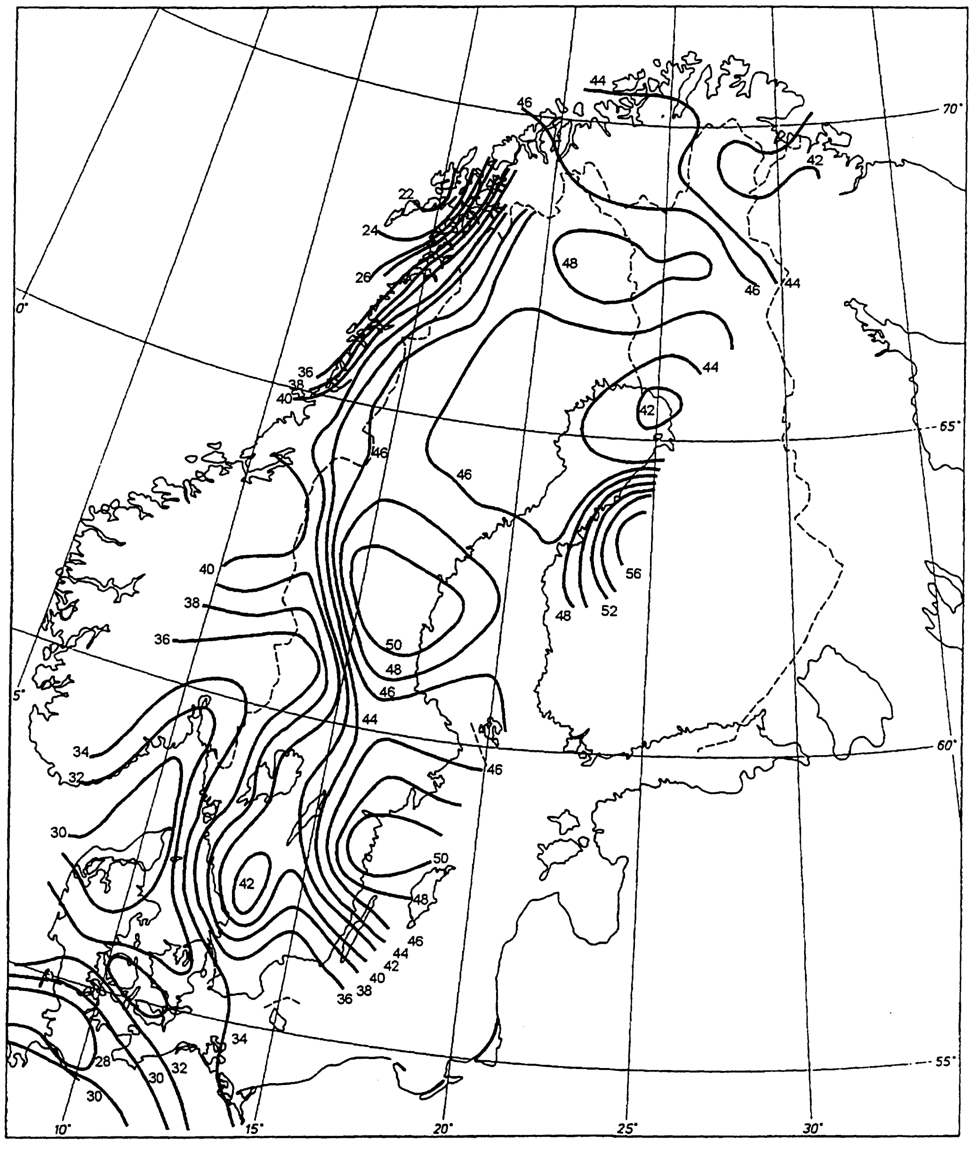

Figure 3-9*. The depth to Moho in km according to Giese & Buness (1992). The map is redrawn.*

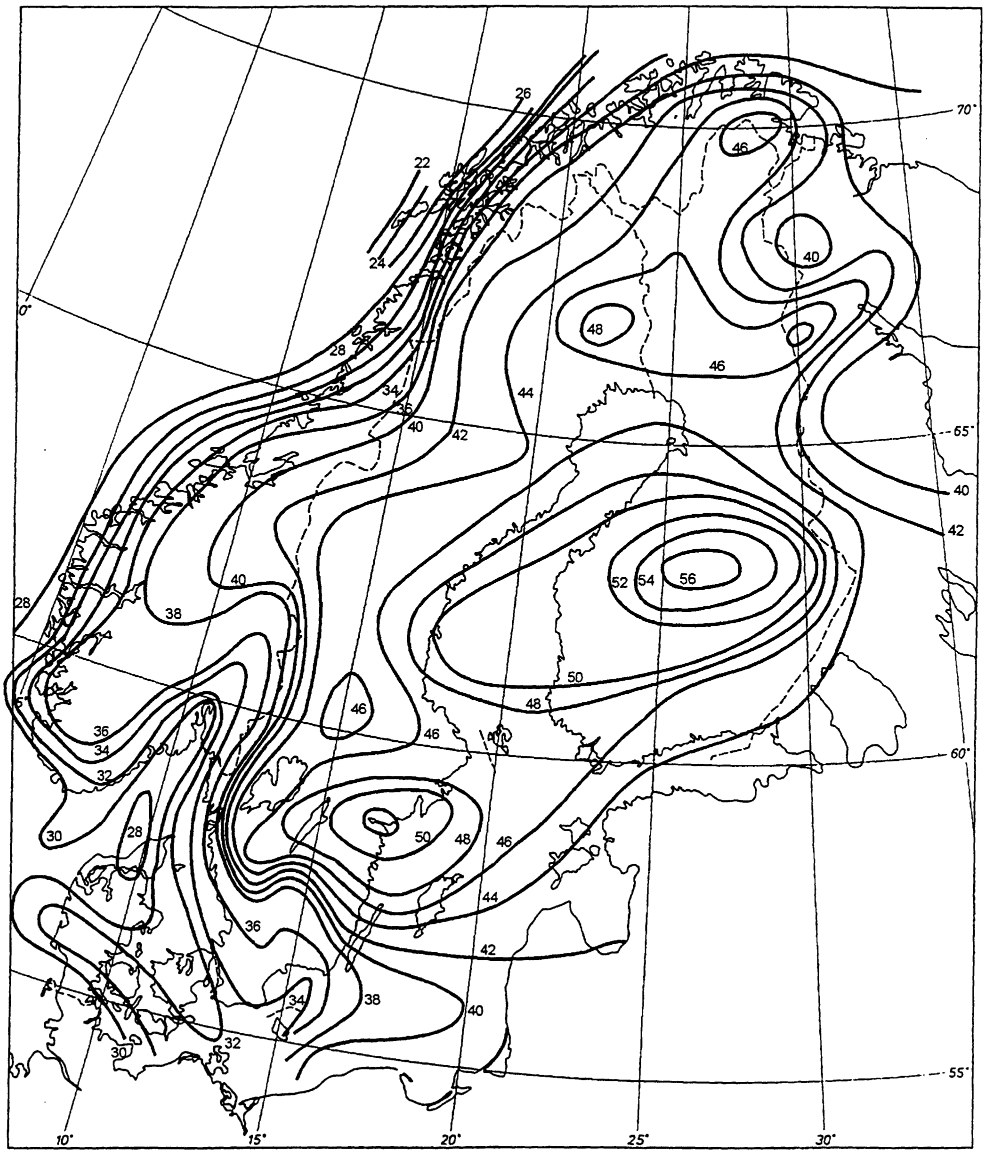

Figure 3-10. *The depth to Moho in km from Kinck et al. (1993).*

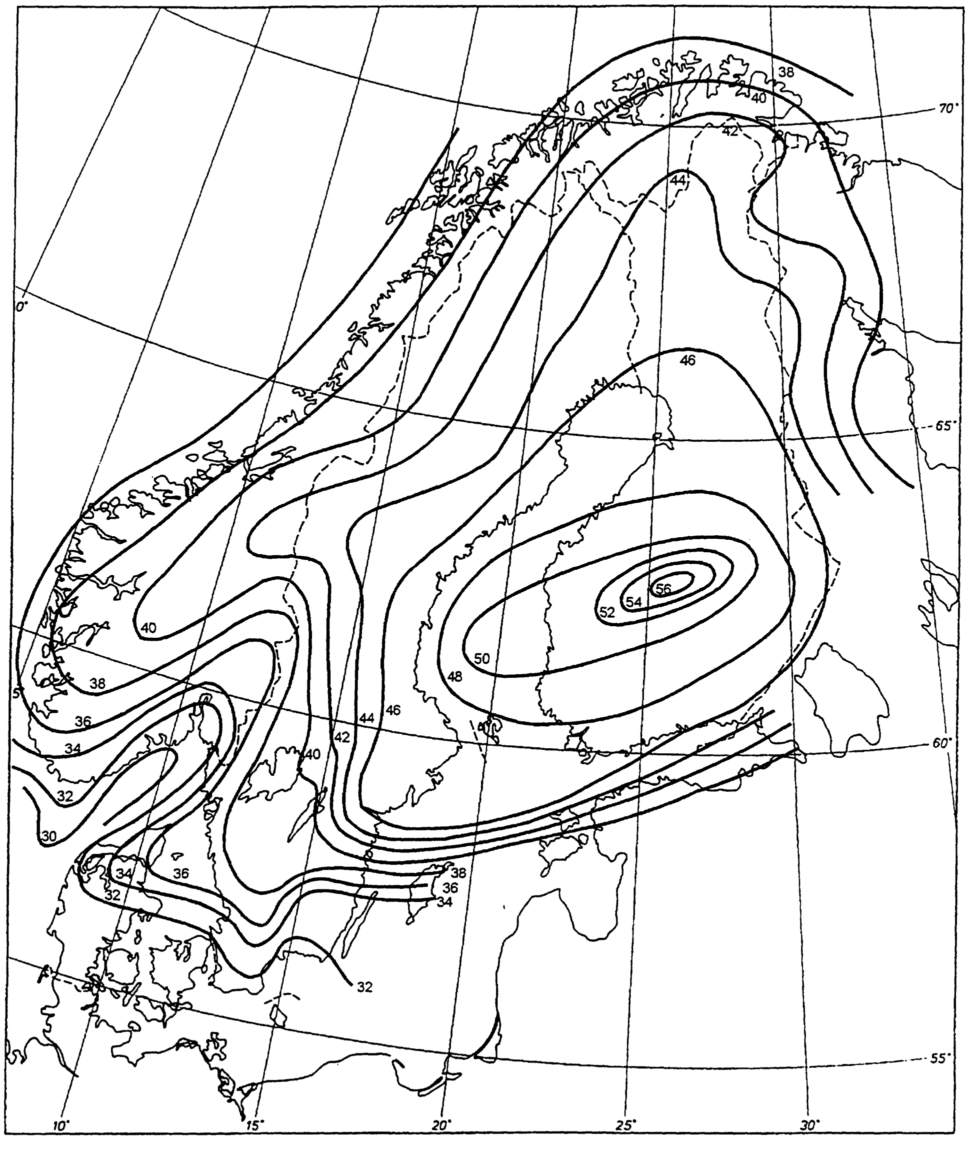

__Figure 3-11__. The depth to Moho in km according to the present model. The values of B_s, corresponding to different crustal thickness, are given in Table 3-3.

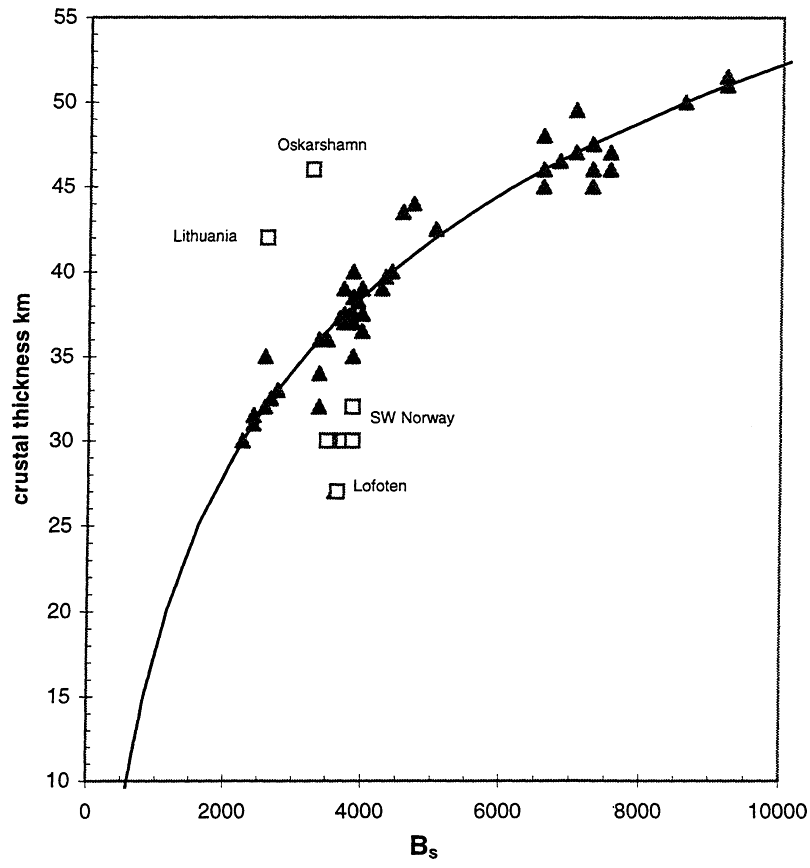

__Figure 3-12__. A comparison between crustal thickness, calculated in the model, and by seismic estimate by either Kinck et al. (1993) or Giese & Buness (1992). The crustal thickness estimated in the model is shown by the curve, which is calculated by formula 3-1. Those seismic estimate which show satisfactory congruence are designated by triangles. The squares designate values which differ. The plot comprises 67 values but some of these coalesce. The good correspondence for most of the sites indicates a relationship between the declining factor and the crustal thickness.

3.2.4 The fast mechanism

Shore level curves, from the area outside the Younger Dryas ice marginal zone at the Norwegian west coast, show a Late Weichselian transgression. The transgression is named the Younger Dryas Transgression and is a result of glacio-isostatic subsidence (Anundsen 1985). A fast subsidence can also be deduced from shore level curves from the northern part of the Swedish west coast. In early Holocene, subsidence was restored by a fast uplift, lasting about 1000 - 2000 years. This fast uplift is deduced from all shore level curves from the central parts of Fennoscandia, while sites in southern Sweden and Denmark were not visibly affected by the fast mechanism. The 17 shore level curves, which indicate fast subsidence followed by fast uplift, are marked by an asterisk in Table 3-2.

Normal distribution functions are used for calculating the fast mechanism. There are some weak indications in the shore level data regarding the fast mechanism, that subsidence occurred more slowly than recovery. However, the normal distribution function is considered to be a sufficient tool for describing the fast mechanism.

The estimated parameters of the fast mechanism are reported in Table 3-2. High values of A_f correspond to high values of B_f. A more careful analysis would possibly give a closer relationship for these parameters. The isolines for the A_f factor, Figure 3-13, show a maximum in that area where the declining rate for the slow mechanism (B_s) is at its lowest, *i.e.* in the area around the Gulf of Bothnia.

The modelling indicates a uniform date of about 11 500 cal years BP (10 300 BP) for T_f, but there are some exceptions which can be seen in Table 3-2. The fast mechanism is visible in shore level curves from sites about 100 km outside the 10 300 BP ice margin. The crustal movement at these sites thus followed a movement created by loading/unloading at least 100 km away.

As mentioned above, Anundsen (1985) proposed, that the Younger Dryas Transgression was a result of glacio-isostatic subsidence caused by the Younger Dryas readvance, which in turn was caused by the climatic deterioration that started about 11 000 BP. This explanation at first seems the most probable interpretation, but several shore level curves show that subsidence started much earlier. The "oldest" curves indicate that it began about 12 500 BP. That means that neither climatic deterioration nor the Younger Dryas readvance are events which triggered the subsidence. On the contrary it is possible that the subsidence triggered the Younger Dryas readvance.

A great part of the slow uplift, especially in central Fennoscandia, occurred before this area finally became free of ice. Because recovery occurred with different velocities the land below the ice sheet was uplifted nonuniformally. In the area around the Gulf of Bothnia the declining rate is relatively much

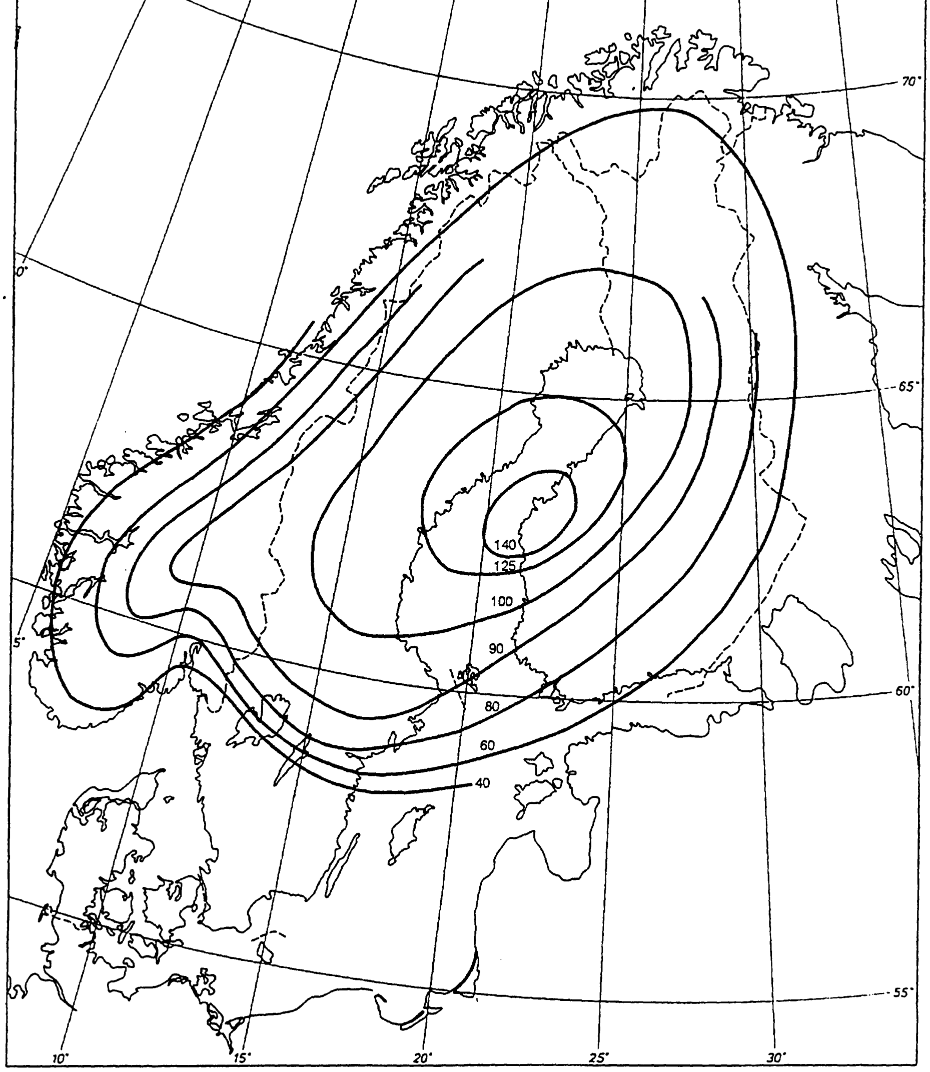

***Figure 3-13**. The values of A_f, i.e. the total subsidence/uplift in m for the fast mechanism.*

lower than in other areas, and recovery in this area was thus delayed. Figure 3-14 shows the difference in slow uplift between Trysil in Norway, representing the centre of ice the dome, and at Lauhanwuori representing the "centre of the subsidence" related to the fast mechanism. The "delay" between these two areas amounts to 270 m for the interval 18 000 - 10 300 BP. If this corresponds to an actual course of events the delay changed the topographical condition below the ice sheet which may have produced "glacial-tilting" analogous to the lake-tilting phenomenon. The glacier ice may then have transgressed the "delayed" areas due to the nonuniform uplift. This hypothesis implies a self-triggered redistribution of the ice load during deglaciation. A glacial transgression may have caused local thickening of the ice sheet, which was compensated by isostatic subsidence, which in turn amplified the process. Climatic deterioration at about 11 000 BP may have further amplified the process with a low deglaciation rate during the cold phase, thus prolonging the period for isostatic delay.

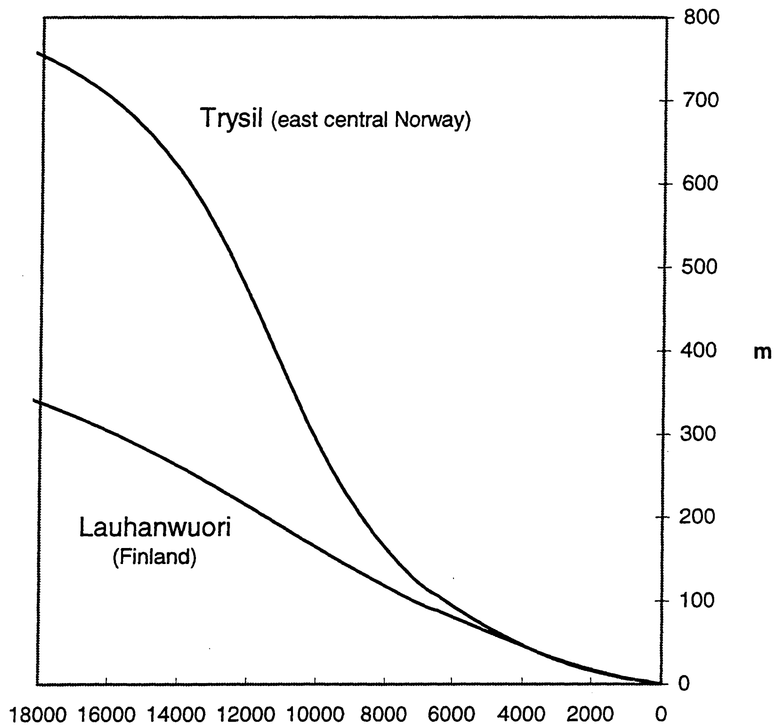

Figure 3-14. Slow uplift at the centre of ice the dome at Trysil in Norway and at Lauhanwuori at the "centre of the subsidence" related to the fast mechanism. The "delay" between these two areas amounts to 270 m for the interval 18 000 - 10 300 BP.

3.2.5 Discussion

Geologists generally describe mantle material as exhibiting plastic behaviour; it behaves like a solid under certain conditions and like a fluid under other conditions. When the material encounters short-lived stresses the material behaves like an elastic solid but in response to long-term stresses it will flow. Ekman & Mäkinen (1996) have proved, by repeated high-precision relative gravity measurements, that a viscous inflow of mantle is a necessary part of the ongoing uplift process. The present uplift is due to a slow mechanism which can be linked to viscous flow and is a response to long-term stresses. The fast mechanism is probably the response to a short-lived stress, which was caused by renewed ice loading, possibly due to the mechanism outlined above. The positions of maximal uplift, related to the slow mechanism and the fast mechanism, are situated at different places. This supports the assumption that these mechanisms are caused by different processes.

During the initial part of crustal recovery the rate of viscous inflow was low even in areas which were already deglaciated. When the inflow to the centre of the depressed dome had reached a maximum, a maximal flow of the mantle material to every spot in the depressed dome is assumed. This process gives a constant value of T_s.

Arctan functions were chosen for calculating glacio-isostatic uplift in this model. The *arctan* function is a symmetrical function where the initial inclining phase of glacio-isostatic uplift is mirrored in the declining phase. This symmetry has most probably given a too simplified picture of the course of uplift during the initial phase when most of the area was still glaciated. A more likely result would probably be obtained for the initial phase if uplift was restrained in some way during this "loaded" phase. However, the *arctan* function seems to fit the empirical information for the declining "unloaded" phase.

As the symmetry of the *arctan* function may probably have given a too simplified picture of uplift for the initial phase, the question arises how much the values of A_s have been affected by this shortcoming. A_s is half of the total uplift (m). If this figure is doubled this would mean the total uplift, but also a doubling of an eventual error. The values of the total uplift should thus be used with caution.

The input data for calculating slow uplift is the crustal thickness and the A_s factor, *i.e.* half of the total uplift in m, which in turn is assumed to be directly proportional to the ice load. The mechanism of slow uplift can thus be regarded as a "simple" mechanical problem.

Mörner (1980a) has presented a map, which has become the conventional picture of the total Fennoscandian uplift. This map is made by assuming glacio-isostatic uplift to start 12 900 BP. The total uplift is then estimated by simply extrapolating the 13 000 year shore lines (!) to an assumed centre of uplift.

Results show that glacio-isostatic uplift is composed of two mechanisms, a proposal earlier put forward by Walcott (1970) who interpreted the uplift with two exponential functions with relaxations times of 1000 and 50 000 years. Walcoot´s (1970) interpretation thus comprises one slow and one fast mechanism. Mörner (1977, 1980a) has also concluded a double nature of Fennoscandian uplift. However, the mechanisms concluded by Mörner (1977, 1980a) are essentially different from the mechanisms presented by the present author. Mörner (1977, 1980a) suggests that uplift since 8 000 BP is predominated by a linear "tectonic" mechanism, while the glacio-isostatic mechanism has been low since 8 000 BP and died out 2 000 - 3 000 years ago.

Most of the uncertainties in the model concern the initial part of the glacio-isostatic uplift. Reliability regarding the latest development is assumed to be satisfactory. This means that most of the discussed uncertainties do not affect the predictions made in Chapter 5.

3.3 SUMMARY OF FORMULAS

Formula for converting dates:

$$t = 59.6\text{-}206.9 \times arctan\ ((4000\text{-}\ 1.095t_{con})/800) + 63.66 \times arctan\ ((7200 -$$

$$- 1.095t_{con})/100)) + 95.5 \times arctan\ ((750 - 1.095t_{con})/200) + 1.095t_{con} \qquad 2\text{-}1$$

where t is the calibrated date, while t_{con} is the conventional radiocarbon date.

Formula for glacio-isostatic uplift (U m):

$$U = 0.6366 \times A_s\ (arctan\ (12\,500 / B_s) - arctan\ ((12\,500 - t) / B_s)) +$$

$$+ A_f \times e^{(-0.5\ (((t - 11\,500)/Bf) \times (t - 11\,500)/Bf)))} \qquad 2\text{-}7$$

where A_s is half of the total uplift (m) for the slow mechanism, A_f is the total subsidence/uplift (m) for the fast mechanism, B_s (y^{-1}) is the declining factor for the slow mechanism, B_f is the declining factor (y^{-1}) for the fast mechanism, and t (year) is the variable time counted in calendar years according to the formula 3-1.

Formula for the main course of eustatic rise (E m):

$$E = 0.6366 \text{ x } 50 \text{ x } (arctan\ (9\,350/1375) - arctan\ ((9\,350 - t)/1375)) \qquad 2\text{-}8$$

Formula for cyclic eustatic changes:

$$C = 0.5 \text{ x } sin\ ((t - 100) \text{ x } 0.013)\text{-}0.48 \qquad 2\text{-}9$$

Formula for the relationship between the declining factor and crustal thickness:

$$B_s = 302\ e^{0.067 * ct} \qquad 3\text{-}1$$

where ct is crustal thickness in km.

4 THE RECENT UPLIFT

Rrecent relative uplift is recorded by precision levellings and tide gauge data. In Finland records are presented by Kääriäinen (1963, 1966) and Suutarinen (1983), in Sweden by RAK (1971, 1974), in Denmark by Simonsen (1969) and Andersen *et al.* (1974), in Norway by Bakkelid (1979). Ekman (1996) has compiled information of the present rate of crustal movements in Fennoscandia mainly from these sources, Figures 4-1, but also in a special map with emphasis on the tide gauge measurements, Figure 4-2.

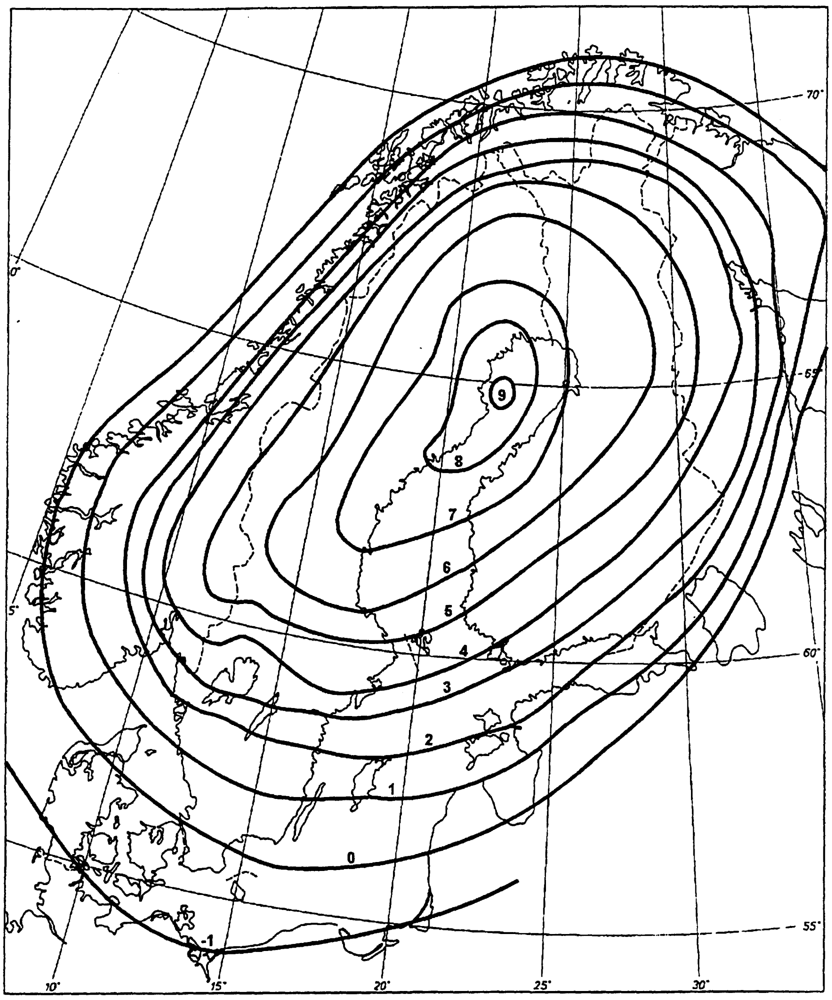

***Figure 4-1**. Recent relative uplift, v_r (mm/ y), recorded by precision levellings and tide gauge data. The map is redrawn from Ekman (1996).*

Recent *relative* uplift recorded by tide gauge data includes eustatic changes. A eustatic rise in the order of 1 mm/ year has been reported, among others by Lizitzen (1974), Mörner (1977, 1980a) and Ekman (1986). Compilations by Emery & Aubrey (1991) and Nakiboglu & Lambeck (1991) indicate a present eustatic rise in the order of 1.2 mm/ year. The first edition (Påsse 1996b) of the modelling includes an analysis of present eustatic rise, which was estimated by subtracting the recent relative uplift (Ekman 1996) from the recent absolute uplift. Recent absolute uplift was calculated at each site used in the modelling. These calculations confirms earlier estimations of an ongoing eustatic rise of about 1.2 mm/y.

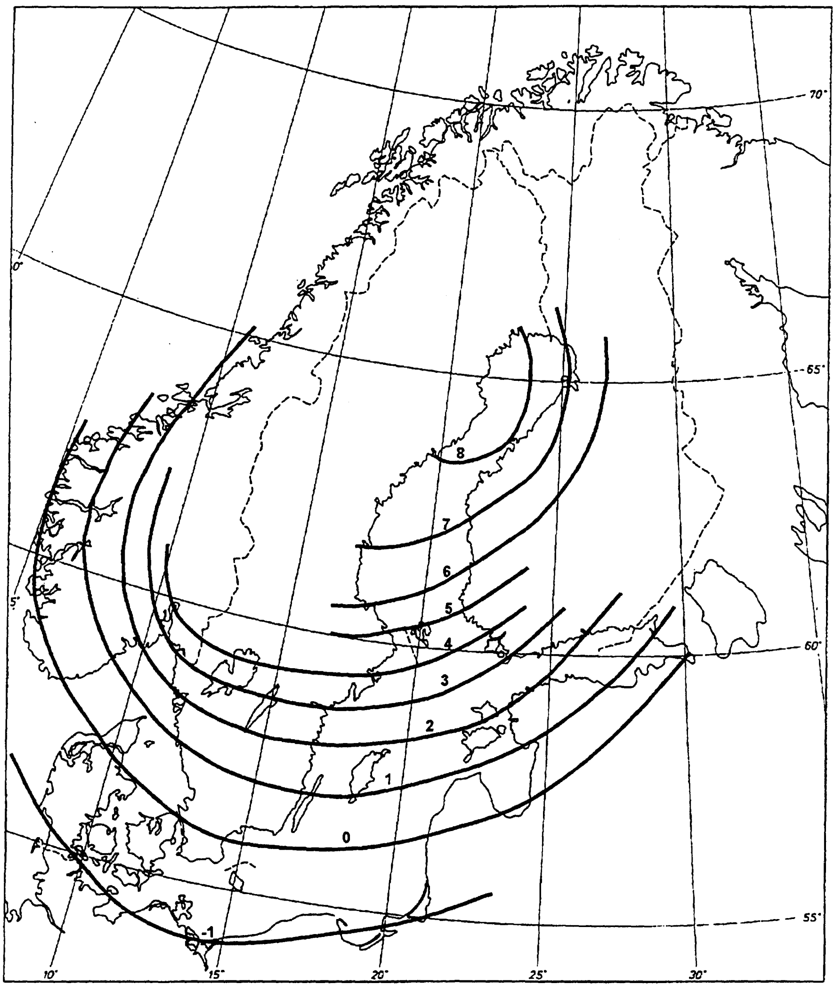

Figure 4-2*. Recent relative uplift, v_r (mm/ y), derived from records of tide gauge data. The map is redrawn from Ekman (1996).*

The isobases of recent relative uplift, recorded by precision levellings (RAK 1971, 1974), obviously reflect the differential declining of the uplift. An example of this is the deviating course of the isobases in the northern part of Bohuslän county and the western part of Värmland county, Figure 4-3. The configuration of the isobases in this area is assumed to reflect the relatively lower decline rate in the western part of Bohuslän county, suggested in the modelling. This example shows that the model can be further improved by utilising detailed information recorded by precision levellings.

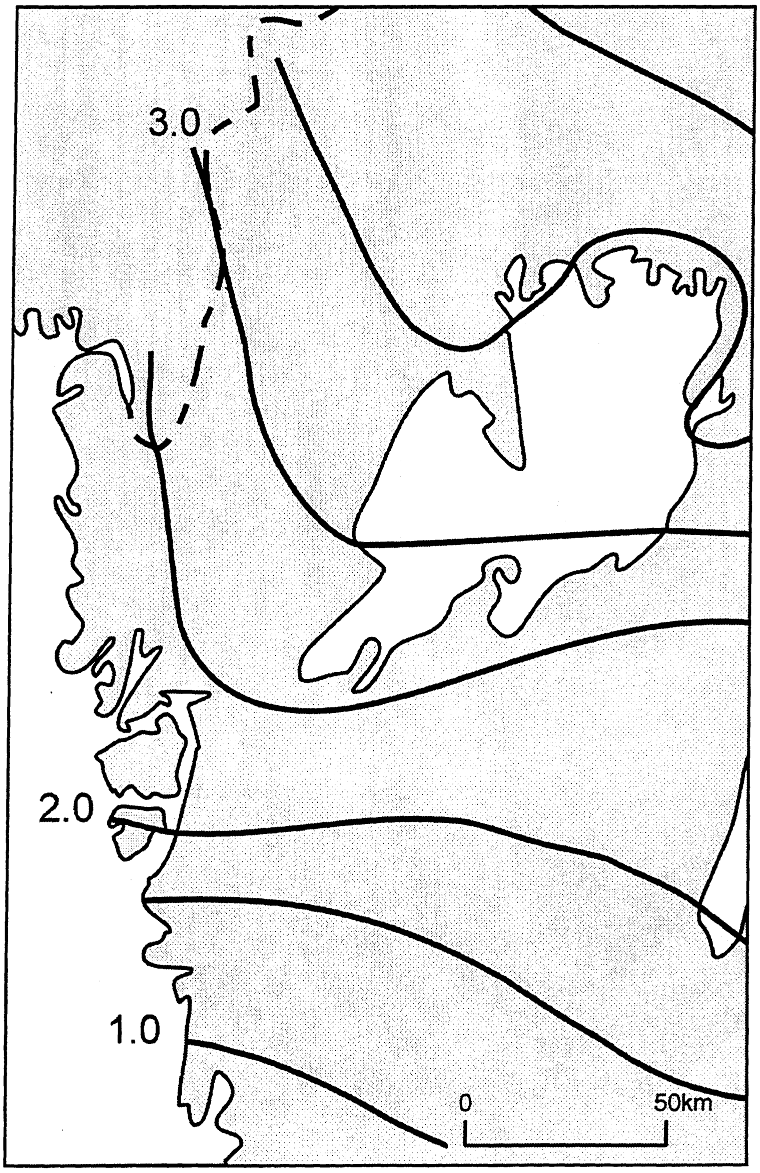

***Figure 4-3**. Isobase map of recent relative uplift (mm/y) in the northern part of Bohuslän county and the western part of Värmland county redrawn from (RAK 1971, 1974). Recent relative uplift is recorded by precision levellings and tide gauge data. The configuration of the isobases is assumed to reflect the relatively lower decline rate in the western part of Bohuslän county, as suggested in the modelling.*

5 THE FUTURE SHORE LEVEL DISPLACEMENT

Future development regarding glacio-isostatic uplift, eustasy and shore level displacement can be predicted in Fennoscandia using the results from the modelling. The predictions are based on the assumption that crustal and eustatic movements follow the trend that exist today. Regarding glacio-isostatic uplift this assumption can most probably be applied as long as no new glaciation starts. Regarding eustatic development it is possible that climatic alterations may change the present eustatic trend. Future glacio-isostatic uplift is thus somewhat easier to predict then eustatic movement and connected shore-level displacement. Future time is designated as negative time in the predictions. Figure 5-1 shows a shore level prediction for Ångermanland extending 100 000 years. This is a too long period for this type of prediction but the intension of this figure is to give a hint of how long glacio-isostatic effects remain after a glacial period.

Predictions at six site in Sweden are shown in Figure 5-2. These predictions are presented in two ways, as curves showing only crustal uplift and as shore-level displacement curves, which include the eustatic trend according to formula 2-9. The predictions extend 10 000 years.

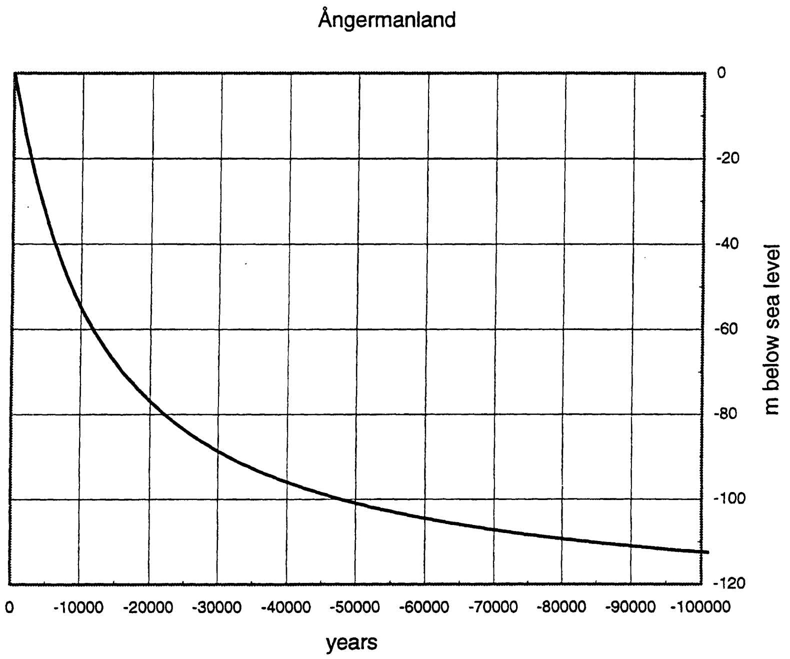

Figure 5-1. Prediction of shore level displacement at Ångermanland extending 100 000 years. Future time is designated as negative time.

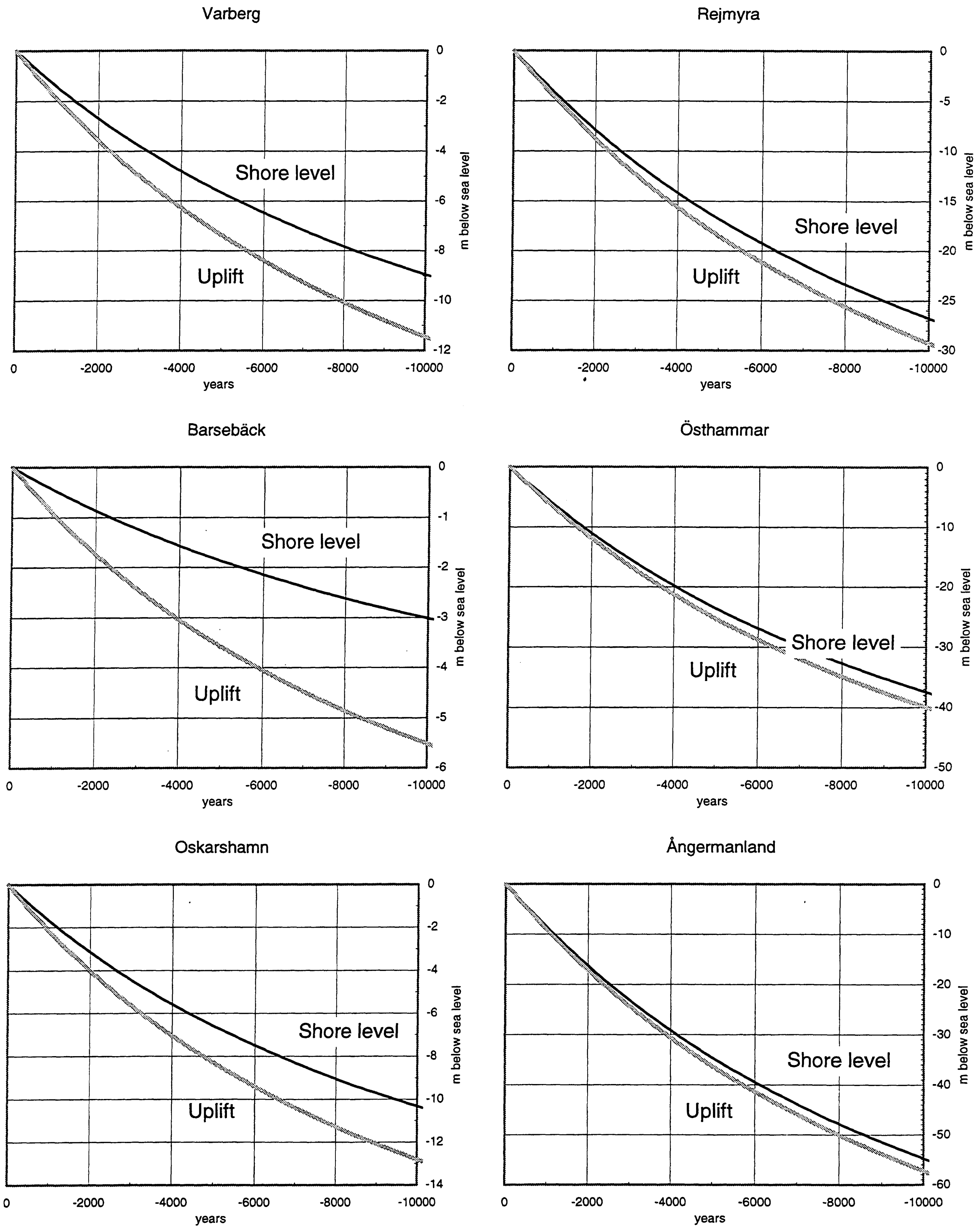

***Figure 5-2**. Predicted shore level displacement, black curve, and glacio-isostatic rise, grey curve, at Varberg, Barsebäck, Oskarshamn, Rejmyra, Östhammar and Ångermanland. The uplift parameters used are in accordance to Table 3-2. The prediction at Östhammar is calculated with A_S= 285 and B_S= 7000.*

6 THE BALTIC

6.1 GENERAL

Shore level curves from the coasts around the Baltic Sea are affected by raised water levels during the two lake stages, the Baltic Ice Lake and the Ancylus Lake. This means that parts of the Baltic shore level curves are not congruous to the marine shore level curves. The differences between the curves can be used for calculating the water level changes and also to deduce the actual thresholds during the different stages of the Baltic, Figure 6-1. The research concerning the development of the Baltic Sea since the last deglaciation has resulted in an immense number of publications. A review of this topic has recently been presented by Björck (1995), which contains most of the relevant references regarding the development of the Baltic Sea.

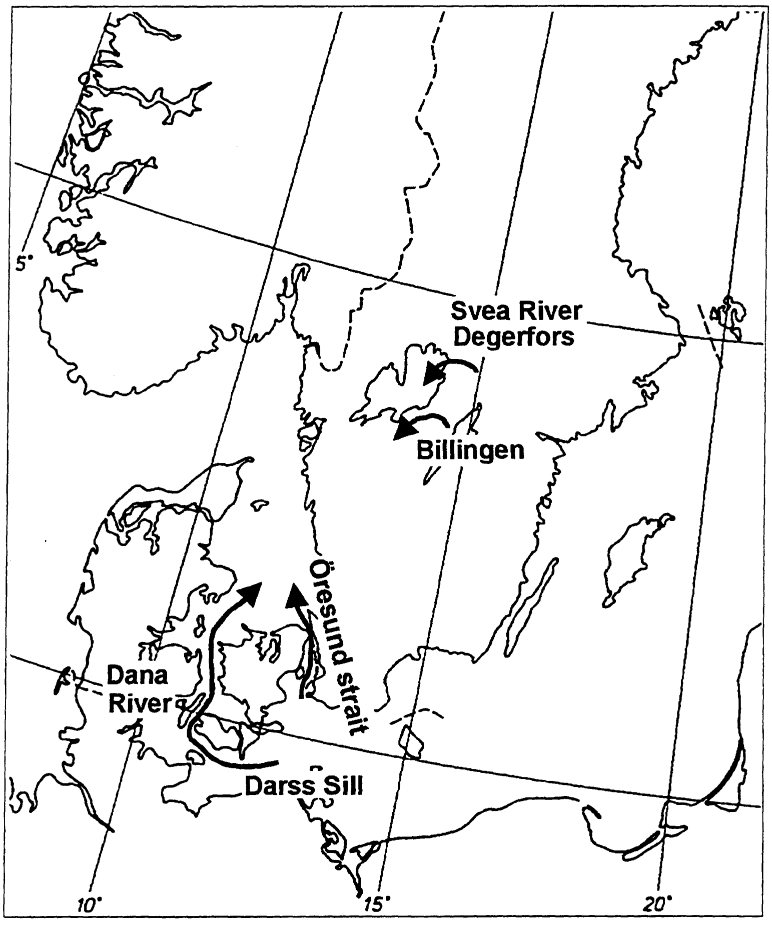

Figure 6-1. The position of the four different outlets that have determined the water level during the different stages of the Baltic basin since the last deglaciation.

6.2 THE BALTIC ICE SEA

The shore level curves from Blekinge and Oskarshamn, Figure 3-5, are the only two curves that comprise the first stage of the Baltic. Comparisons between these curves and calculated curves of the corresponding marine shore level displacement, show that the water level within the Baltic basin, until 12 000 ± 100 BP, was in level with the sea. The shore level displacement in the southern part of the Öresund Strait, where a threshold exists at about -7 m, is shown in Figure 6-2. The shore level curve indicates that this threshold was isolated about 12 000 BP. A sea facies at the beginning of the development of the Baltic has been proposed by Nilsson (1968) who names this stage the Baltic Ice Sea.

6.3 THE BALTIC ICE LAKE

After the isolation 12 000 ± 100 BP the water level in the Baltic increased due to the uplift (the shore level displacement) of the threshold. The difference between the water level of the Baltic and the sea can be calculated by using the shore level curve from Oskarshamn, Figure 3-5. These values are plotted in Figure 6-3 and compared to the calculated rate of the shore level displacement at the threshold at Öresund. This figure shows that the water level rise at Oskarshamn most probably is related to the raised threshold at Öresund. The increase of the water level in the Baltic Ice Lake continued until approximately 10 400 ± 100 BP, when the opening of a threshold in the Billingen area caused a catastrophic drainage. Before that the water level in the Baltic had reached about 26 m above sea level according to Figure 6-3. This theoretical discussion of the development presuppose that the Darss Sill do not yet exist. This threshold is thus assumed to have been formed by erosion in a later stage.

6.4 THE YOLDIA SEA

After the drainage of the Baltic Ice Lake the shore level in the Baltic followed the marine water level about 800 - 1000 years. Due to the crustal uplift there was a fast gradual lowering of the connection between the Baltic and the sea. The Yoldia Sea thus became an inland sea during the latter part of this stage. This stage ended when the threshold at Degerfors was emerged about 9 600 ± 100 BP, Figure 6-2.

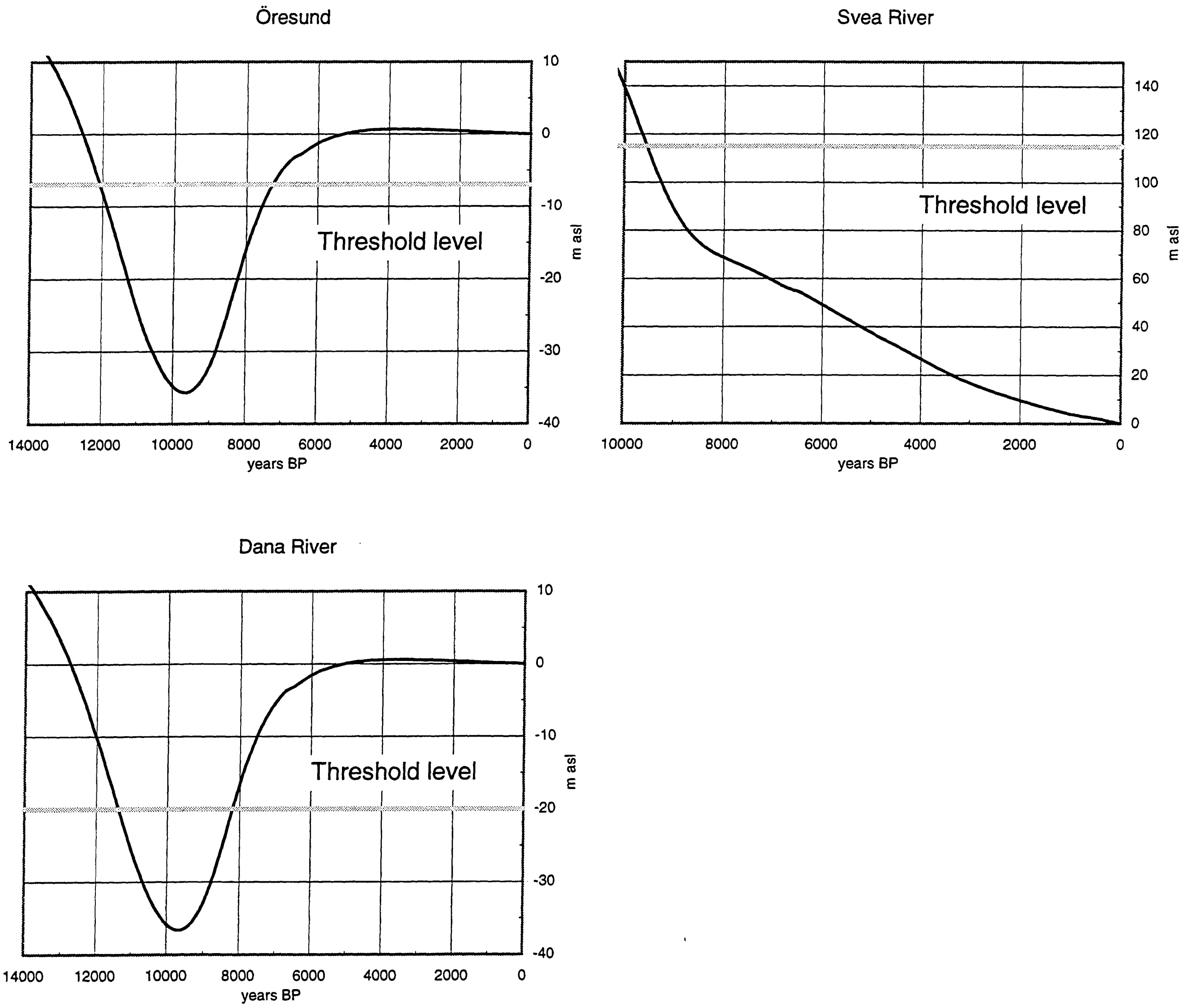

Figure 6-2*. Calculated shore level curves at Öresund, Dana River and Svea River. The grey lines designates the levels of the thresholds. The threshold at Dana River (Darss Sill) is assumed to have been dammed by at least 10 m of quaternary deposits at 12 000 BP.*

6.5 THE ANCYLUS LAKE

A very fast transgression, the Ancylus transgression, started in the Baltic when the threshold at Degerfors was isolated and the Baltic was drained by the Svea River. The rise of the water level within the Baltic followed the rise of the threshold at Degerfors, which was very fast during this period. The rise of the threshold at Degerfors is calculated with A_s = 295, B_s = 4400, A_f = 45, and B_f = 1000. This rise is shown in Figure 6-4. The exact time of the isolation at Degerfors is unknown. In Figure 6-4 the transgression is assumed to have started 9 600 BP. When the water level, after a transgressive phase of about 300 years, had reached a level of about 15 m a new outlet, the Dana River, was opened in the southern part of the Baltic. This alteration of the outlet occurred about 9 300 BP, a date which also represents the maximum of the Ancylus transgression. After this maximum the water level of the Baltic decreased in phase with the shore level displacement at the Darss Sill, Figure 6-2. This stage may be named the Ancylus regression. The threshold at Dana River was reached by the marine transgression at about 8 200 BP, Figure 6-2. This date defines the end of the Ancylus Lake.

6.6 THE LITORINA SEA

The sea intruded the Baltic through the Storebält (the Great Belt) about 8200 BP. The Baltic was once again on a level with the sea. About 1000 years later a connection to the sea also was opened through the Öresund strait. This stage of the Baltic is named the Litorina Sea. The initial phase of the Litorina Sea is commonly considered to be a separate stage, the Mastogloia Sea. This sub-stage is defined by brackish conditions, caused by the shallow connections between the sea and the Baltic during this time. The changes of the water level of the Baltic since the last deglaciation are summarised in Figure 6-5.

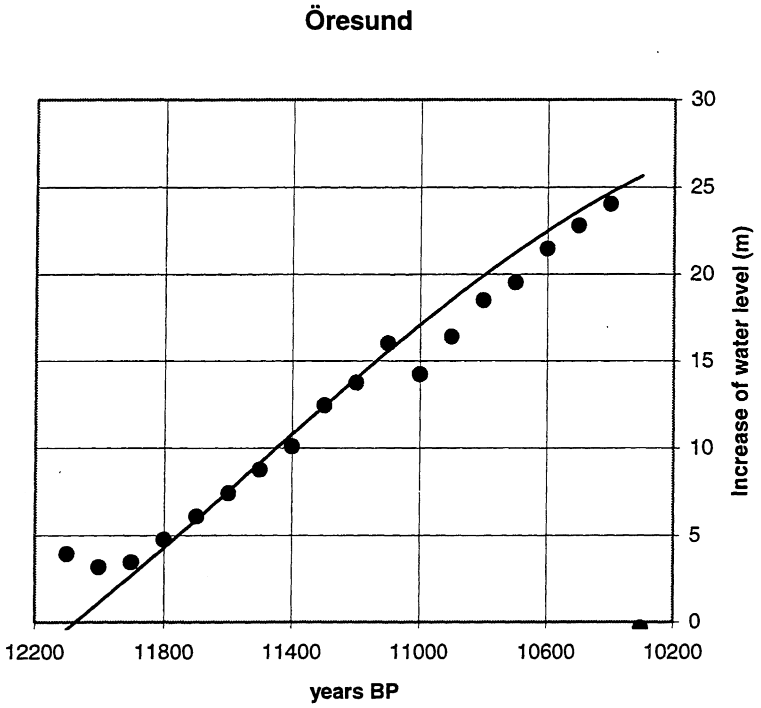

Figure 6-3. The water level rise in the Baltic Ice Lake. The water level rise recorded at Oskarshamn is shown with dots. This rise is related to the calculated rate of shore level displacement at the threshold at Öresund, black line. The transgression in the Baltic Ice Lake continued to about 10 400 ± 100 BP and reached a level of about 26 m before the drainage.

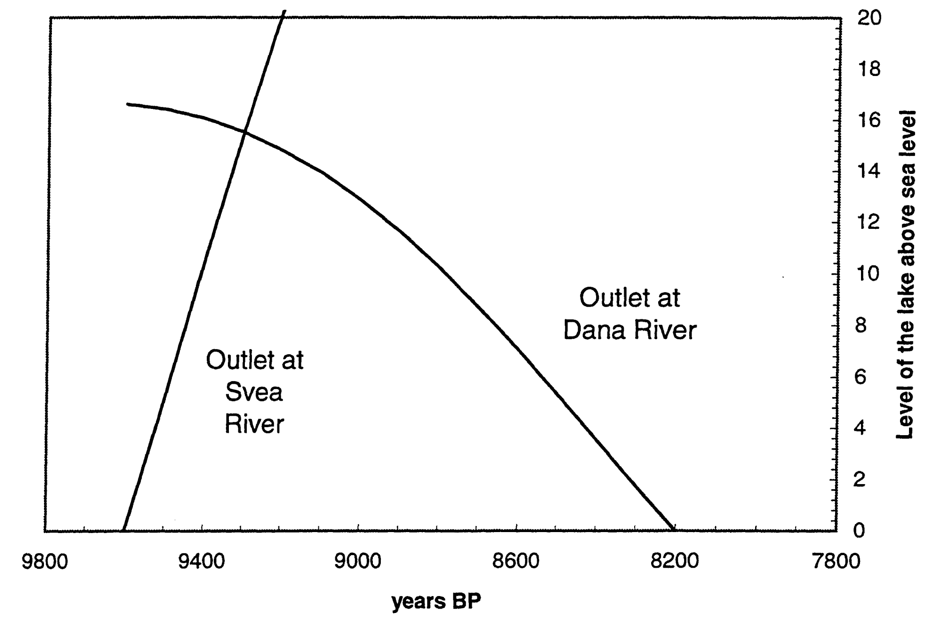

Figure 6-4. The water level changes during the Ancylus Lake are estimated by combining the results of the calculated shore level displacements at the outlets at Svea River and Dana River.

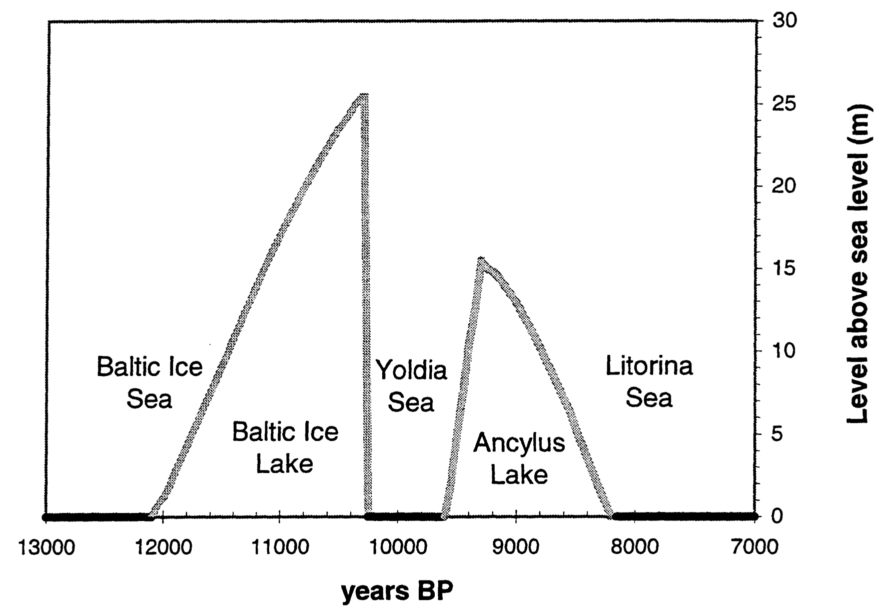

Figure 6-5 Calculated changes of the water level of the Baltic.

REFERENCES

Andersen O. B., Kejlsö E. & Remmer O. 1974. Secular movements within Jutland as determined from repeated precise levellings. Geodaet. Inst. Skr. 3. rk. 40. 1 - 70.

Andrews J.T. 1970. A Geomorphological Study of Post-Glacial Uplift, with Particular Reference to Arctic Canada: Institute of British Geographers. Special Publication No. 2., 1-156.

Anundsen K. 1985. Changes in shore-level and ice-front position in Late Weichselian and Holocene, southern Norway. Norsk Geografisk Tidskrift 39, 205 - 225.

Åse L.-E. 1970. Kvartärbiologiska vittnesbörd om strandförskjutningen vid Stockholm under de senaste c. 4000 åren. Geologiska Föreningens i Stockholm Förhandlingar 92, 49 - 78.

Asklund B. 1935. Gästrikländska fornstrandlinjer och nivåförändringsproblemen. Sveriges geologiska undersökning C 391, 1 - 119.

Bakkelid S. 1979. Et forelöpig totalbilde av landhevningen i Norge. Norges Geografiske Oppmålning, 1- 22.

Bennike O. & Jensen J. B. 1995. Near-shore Baltic Ice Lake deposits in Fakse Bugt, southeast Denmark. Boreas 24, 185-195.

Berglund M. 1995. The Late Weichselian deglaciation, vegetational development and shore displacement in Halland, southwestern Sweden. University of Lund, Department of Quaternary Geology, Thesis 35, 1 - 113.

Bird E. C. F. & Klemsdal T. 1986. Shore displacement and the origin of the lagoon at Brusand, southwestern Norway. Norsk Geografisk Tidskrift 40, 27 - 35.

Björck S. 1979. Late Weichselian stratigraphy of Blekinge, SE Sweden, and water level changes in the Baltic Ice Lake. University of Lund, Department of Quaternary Geology, Thesis 7, 1 - 248.

Björck S. 1995. A reviw of the history of the Baltic Sea, 13.0-8.0 ka BP. Quaternary International 27, 19 - 40.

Björck S. & Digerfeld G. 1982. Late Weichselian shore displacement at Hunneberg, southern Sweden, indicating complex uplift. Geologiska Föreningens i Stockholm Förhandlingar 104, 132 - 155.

Björck S. & Digerfeld G. 1991. Alleröd- Younger Ryas sea level changes in southwestern Sweden and their relation to the Baltic Ice Lake development. Boreas 20, 115 - 133.

Bloom A.L. 1967. Pleistocene shorelines: a new test of isostasy. Geol. Soc. Am. Bull. 78, 1477-1494.

Brunnberg L., Miller U. & Risberg J. 1985. Project Eastern Svealand: Development of the Holocene landscape. ISKOS 5, 85 - 91.

Caldenius C. & Linman G. 1949. En senkvartär regressions- och transgressionslagerföljd vid Halmstad. Sveriges geologiska undersökning C 502, 1 - 26.

Caldenius C., Larsson W., Mohrén E., Linman G. & Tullström H. 1966. Beskrivning till kartbladet Halmstad. Sveriges geologiska undersökning Aa 198, 1-138.

Cato I. 1992. Shore displacement data based on lake isolations confirm the postglacial part of the Swedish Geochronological Time Scale. Sveriges geologiska undersökning Ca 81, 75 - 80.

Cathles L. M. 1975. The viscosity of the earth's mantle. Princeton University Press, Princeton, New Jersey,1-386.

Celsius A. 1743. Anmärkning om vatnets förminskande så i Östersiön som Vesterhafvet. Kongl. Swenska Wetenskaps Academiens Handlingar 4, 33-50.

Clark R. D., Farrell W. E. & Peltier W. R. 1978. Global changes in postglacial sea level: a numerical calculation. Quaternary Research 9: 265 - 278.

Christensen C. 1993. Land and sea. In: Hvass & Stovgaard (eds). Digging into the past - 25 years of Archaeology in Denmark. Aarhus Universitetsforlag, 20-23.

Daly R. A. 1934. The Changing World of the Ice Age. Hafner, New York, 1 - 271.

Danielsen A. 1970. Pollen-analytical Late-Quaternary studies in the Ra district of Östfold, southeast Norway. Årsbog for universitetet i Bergen, mat.-naturv. serie 1969:14, 1-143.

Digerfeldt G. 1975. A standard profile for Littorina transgression in western Skåne, South Sweden. Boreas 4, 125 - 142.

Donner J. 1980. The detemination and dating of synchronous Late Quaternary shorelines in Fennoscandia. In: N.A. Mörner (Ed.), Earth Rheology, Isostasy and Eustasy. Wiley, New York; N.Y, 285 - 293.

Ekman M. 1986. A reinvestigation of the world's second longest eries of sea level observations: Stockholm 1774 - 1984. National Land Survey of Sweden, Professional Papers 1986:4.

Ekman M. 1996. A Consistent Map of the Postglacial Uplift of Fennoscandia. Terra Nova 8, 158 - 165.

Ekman M. & Mäkinen J. 1996. Recent postglacial rebound, gravity change and mantle flow in Fennoscandia. Geophysical Journal International 126, 229-234.

Emery K. O. & Aubrey D. G. 1991. Sea levels, land levels, and tide gauges. Springer-Verlag, 1-237.

Eronen M. 1976. A radiocarbon-dated Ancylus transgression site in south-eastern Finland. Boreas 5, 65 - 76.

Eronen M. 1983. Late Weichselian and Holocene shore displacement in Finland. In D.E. Smith & G. Dawson (eds.): Shorelines and Isostasy. Institute of British Geographers, Special Publication 16, Academic Press, 1983, 183-207.

Eronen M. & Haila H. 1982. Shorelines displacement near Helsinki, southern Finland, during the Ancylus Lake stage. Annales Academiae Scientiarum Fennicae AIII 134, 111 - 129.

Eronen M., Glückert G., van de Plassche O., van der Plicht J. & Rantala P. 1995. Land uplift in the Olkiluoto-Pyhäjärvi area, southwestern Finland, during the last 8 000 years. Nuclear Waste Commission of Finnish Power Companies, Report YJT-95-17, 1- 26.

Fairbanks R.G. 1989. A 17, 000- years glacio-eustatic sea lrvel record: influence of glacial melting rates on the Younger Dryas event and deep- ocean circulation. Nature 342, 637 - 642.

Fairbridge R.W. 1961. Eustatic changes in sea level. Physics and Chemistry of the Earth 4, 99-185.

Fjeldskaar W. & Cathles L. 1991. Rheology of mantle and lithosphere inferred from post-glacial uplift in Fennoscandia. In: Sabdini *et al.* (eds): Glacial isostasy, sea-level and mantle rheology, Kluwer Academic Publishers, 1 - 19.

Giese P. & Buness H. 1992. Moho depth. In. A continent revealed. The European Geotraverse. Atlas of Compiled Data. R. Freeman & S. Mueller (eds.), Cambridge University Press, 11- 13.

Glückert G. 1976. Post-glacial shore-level displacement of the Baltic in SW Finland. Annales Academiae Scientiarum Fennicae AIII 134, 1 - 92.

Glückert G. 1978. Östersjöns postglaciala strandförskjutning och skogens historia på Åland. Publication Department of Quaternary Geology, University of Turku, 1 - 106.

Glückert G. & Ristaniemi O. 1982. The Ancylus transgression west of Helsinki, South Finland - A preliminary report. Annales Academiae Scientiarum Fennicae AIII 134, 99 - 134.

Godwin H., Suggate R. P. & Willis E. H. 1958. Radiocarbon dating of the eustatic rise in ocean-level. Nature 181, 1518 - 1519.

Hafsten U. 1983. Shore-level changes in South Norway during the last 13,000 years, traced by biostratigraphical methods and radiometric datings. Norsk Geografisk Tidskrift 37, 63 - 79.

Hald M. & Vorren T. O. 1983. A shore displacement curve from the Tromsö district, North Norway. Norsk Geologisk Tidskrift 63, 103 - 110.

Helle S.K., Anundsen K., Aasheim S. & Hafildason H. 1997. Indications of a younger Dryas marine transgression in inner Hardanger, West Norway. Norsk Geologisk Tidskrift 77, 101 - 117.

Henningsmoen K. E. 1979. En karbon-datert strandforskyvningskurve fra söndre Vestfold. 239 - 247. In. Nydal, R., Westin, S., Hafsten, U. & Gulliksen, S.: Fortiden i sökelyset. Trondheim. (Univ. forl.)

Hyvärinen H. 1980. Relative sea-level changes near Helsinki, southern Finland during early Litorina times. Bullentin of the Geological Society of Finland 52, 207 - 219.

Hyvärinen H. 1984. The Mastogloia stage in the Baltic Sea history: Diatom evidence from southern Finland. Bullentin of the Geological Society of Finland 56. 1-2, 99 - 115.

Jelgersma S. 1961. Holocene sea level changes in the Netherlands. Meded. Geol. Sticht., C, VI, 7. 1-100.

Kääriäinen E. 1963. Land uplift in Finland computed by aid of precise levellings. Fennia 89, 15 - 19.

Kääriäinen E. 1966. The second levelling of Finland in 1935 - 1955. Veröff. Finn. Geodät. Inst. 61, Helsinki, 1 - 331.

Kabailiene M. 1997. Shore line displacement, palaeoecological conditions and human impact on the southeastern coast of Baltic sea. In: The fifth marine geological conference "The Baltic", A. Gregelis (ed.), 114 - 122. Lihuanian Institute of Geology. Vilinius 1997.

Kaland P. E. 1984. Holocene shore displacement and shorelines in Hordaland, western Norway. Boreas 13, 203 - 242.

Kaland P. E., Krzywinski, K. & Stabell B. 1984. Radiocarbondating of the transitions between marine and lacustrine sediments and their relation to the development of lakes. Boreas 13, 243 - 258.

Kessel H. & Raukas A. 1979. The Quaternary History of the Baltic, Estonia. In: V. Gudelis & L.-K. Königsson (eds), The Quaternary History of the Baltic, 127 - 146. Acta Universitatis Upsaliensis Symposia Universitatis Upsaliensis Annum Quingentesimum Celebrantes 1. Uppsala

Kinck J. J., Husebye E. S. & Larsson F. R. 1993. The Moho depth distribution in Fennoscandia and the regional tectonic evolution from Archean to Permian times. Precambrian Research, 64, 23 - 51.

Kjemperud A. 1986. Late Weichselian and Holocene shore displacement in the Trondheimsfjord area, central Norway. Bores 15, 61 - 82.

Klug H. 1980. Der Anstieg des Ostseespiegels im deutchen Küstenraum set dem Mittelatlantikum. Eiszeitalter und Gegenwart 30, 237 - 252.

Krzywinski K. & Stabell B. 1984. Late Weichselian sea level changes at Sotra, Hordaland, western Norway. Boreas 13, 159 - 202.

Lambeck K. 1991. A model for Devensian and Flandrian glacial rebound and sea-level change in Scotland. In: Sabdini *et al.* (eds): Glacial isostasy, sea-level and mantle rheology, Kluwer Academic Publishers, 33-61.

Liljegren R. 1982. Paleoekologi och strandförskjutning i en Littorinavik vid Spjälkö i mellersta Blekinge. University of Lund, Department of Quaternary Geology, Thesis 11, 1 - 95.

Lisitzin E. 1974. Sea-level changes. Elsevier Scientific Publishing Co. 1974.

Lundqvist G. 1962. Geological radiocarbon datings from the Stockholm station. Sveriges geologiska undersökning C 589, 1 - 23.

McConnell R. K. 1968. Viscosity of the Mantle from Relaxation Time Spectra of Isostatic Adjustment: J. Geophys. Res.73, 7089-7105.

Meissner R., Wever Th. & Flüh E.R. 1987. The Moho in Europe - Implications for crustal development. Annales Geophysicae, 357 - 364.

Miller U. & Robertsson A.-M. 1982. The Helgeandsholmen excavation: An outline of biostratigraphical studies to document shore displacement and vegetational changes. PACT 7, 311 - 327.

Miller U. & Robertsson A.-M. 1988. Late Weichselian and Holocene environmental changes in Bohuslän, Southwestern Sweden. Geographia Polonica 55, 103 - 111.

Möller J. J. 1984. Holocene shore displacement at Nappstraumen, Lofoten, North Norway. Norsk Geologisk Tidskrift 64, 1 - 5.

Mörner N. A. 1976. Eustatic changes during the last 8,000 years in view of radiocarbon calibration and new information from the Kattegatt region and other northwestern European coastal areas. Palaeogeography, Palaeoclimatology, Palaeoecology, 19, 63 - 85.

Mörner N. A. 1977. Past and present uplift in Sweden glacial isostasy, tectonism and bedrock influence. Geologiska Föreningens i Stockholm Förhandlingar 99, 48 - 54.

Mörner N. A. 1980a. The Fennoscandian Uplift: Geological Data and their Geodynamical Implication. In: Earth Rheology, Isostasy, and Eustasy. Ed. N.-A. Mörner. Avon, 251 - 283.

Mörner N. A. 1980b. The Northwest European " sea -level laboratory" and regional Holocene eustasy. Palaeogeography, Palaeoclimatology, Palaeoecology, 29, 281 - 300.

Nakada M. & Lambeck K. 1987. Glacial rebound and relative sea-level variations: a new appraisal. Geophysical Journal Royal Astronomical Society 90, 171 - 224.

Nakada M. & Lambeck K. 1989. Late Pleistocene and Holocene sea-level change in the Austrailian region and mantle rheology. *Geophysical Journal 96.* 497 - 517.

Nakiboglu S. M. & Lambeck K. 1991. Secular sea-level change. *In:* Sabdini *et al.* (eds): Glacial isostasy, sea-level and mantle rheology, Kluwer Academic Publishers, 237-258.

Nilsson E. 1968. Södra Sveriges senkvartära historia. Geokronologi, issjöar och landhöjning. Kungliga Svenska Vetenskapsakademiens Handlingar. Fjärde serien. Band 12. Nr 1, 1 - 117.

Påsse T. 1983. Havsstrandens nivåförändringar i norra Halland under Holocen tid. Göteborgs universitet. Geologiska institutionen A 45,1 - 174.

Påsse T. 1986. Beskrivning till jordartskartan Kungsbacka SO. Sveriges geologiska undersökning Ae 56, 1 - 106.

Påsse T. 1987. Shore displacement during the Late Weichselian and Holocene in the Sandsjöbacka area, SW Sweden. Geologiska Föreningens i Stockholm Förhandlingar 109, 197 - 210.

Påsse T. 1988. Beskrivning till jordartskartan Varberg SO/ Ullared SV. Sveriges geologiska undersökning Ae 86, 1 - 98.

Påsse T. 1990a. Emperical estimation of isostatic uplift using the lake-tilting method at Lake Fegen and at Lake Säven, southwestern Sweden. Mathematical Geology 22, No. 7, 803 - 824.

Påsse T. 1990b. Beskrivning till jordartskartan Varberg NO. Sveriges geologiska undersökning Ae 102, 1 - 117.

Påsse T. 1996a. Lake-tilting investigations in southern Sweden. SKB Technical Report 96-10, 1 - 34.

Påsse T. 1996b. A mathematical model of the shore level displacement in Fennoscandia. SKB Technical Report 96-24, 1 - 92.

Peltier W. R., 1976. Glacial isostatic adjustments - II: The inverse problem. Geophysical Journal Royal Astronomical Society 46, 605 -646.

Peltier W. R. 1988. Lithospheric thickness, Antarctic deglaciation history, and ocean basin discretization effect in a global model of postglacial sea level changes: a summary of some sources of nonuniqueness. Quaternart Reaserch 29. 93 - 112.

Peltier W. R. 1991. The ICE-3G model of late Pleistocene deglaciation: construction, verification, and applications. In: R. Sabadini et al. (Editors), Glacial,Isostasy, Sea-level and Mantle Rheology. Kluwer, Dordrecht, 95 - 119.

Persson C. 1979. Shore displacement during Ancylus time in the Rejmyra area, south central Sweden. Sveriges geologiska undersökning C 755, 1 - 23.

Persson G. 1962. En transgressionslagerföljd från Limhamn. Geologiska Föreningens i Stockholm Förhandlingar 84, 47 - 55.

Persson G. 1973. Postglacial transgressions in Bohuslän, Southwestern Sweden. Sveriges geologiska undersökning C 684, 1 - 47.

RAK (Rikets allmänna kartverk) 1971. Geodetic activities in Sweden 1967-1970. Geographical Survey Office of Sweden A 38, 1 - 19.

RAK (Rikets allmänna kartverk) 1974. Sveriges andra precisionsavvägning 1951-1967. Geographical Survey Office of Sweden A 40, 1-91.

Ramfjord H. 1982. On the Late Weichselian and Flandrian shoreline displacement in Naeröy, Nord-Tröndelag, Norway. Norsk Geologisk Tidskrift 62, 191 - 205.

Renberg I. & Segerström U. 1981. The initial points on a shoreline displacement curve for southern Västerbotten, dated by varve-counts of lake sediments. Striae 14, 174 - 176.

Richardt N. 1996. Sedimentological examination of the Late Weichselian sea-level history following deglaciation of northern Denmark. Geological Society Special Publication 111, 261 - 273.

Ringberg B. 1989. Upper Late Weichselian lithostratigraphy in western Skåne, southernmost Sweden. Geologiska Föreningens i Stockholm Förhandlingar 111, 319 -337.

Risberg J. 1991. Palaeoenvironment and sea level changes during the early Holocene on the Södertörn penisula, Södermanland, eastern Sweden. Stockholm University, Department of Quaternary Research. Report 20, 1 - 27.

Robertsson A. -M. 1991. Strandförskjutningen i Eskiltunatrakten för ca 9 000 till 4 000 år sedan. Sveriges geologiska undersökning, Rapporter och meddelanden 67, 1 - 27.

Saarnisto M. 1981. Holocene emergence history and stratigraphy in the area north of the Gulf of Bothnia. Annales Academiae Scientiarum Fennicae AIII 130, 1 - 42.

Salomaa R. 1982. Post-glacial shoreline displacement in the Lauhanvuori area, western Finland. Annales Academiae Scientiarum Fennicae AIII 134, 81 - 97.

Salomaa R. & Matiskainen H. 1983. Rannan siirtyminen ja arkeologinen kronologia Etelä-Pohjanmaalla. Arkeologian päivät 7 -8.4. 1983 Lammin Biolog. tutkimusasemalla. Karhunhammas 7, 21 - 36.

Salonen V. - P., Räsenen M. & Terho A. 1984. Palaeolimnology of ancient Lake Mätäjärvi. Third Nordic Conference on the application of scientific methods in archaelogy. Mariehamn, Åland, Finland, 8-11. October 1984. Iskos 5, 233 - 288.

Sandegren R. & Johansson H. E. 1931. Beskrivning till kartbladet Göteborg. Sveriges geologiska undersökning Aa 173, 1 - 141.

Shepard F. P. 1963. Submarine Geology. Harper and Row, New York, N.Y. 2nd ed., 1-557.

Simonsen O. 1969. Some remarks in May 1968 on the secular movements within Denmark. In. J. A. Mescherikov, Problems of recent crustal movements of the Earth, USSR Acad. Sci., Moscow.

Snyder J.A., Korsun S.A. & Forman S.L. 1996. Postglacial emergence and Tapes transgression, north-central Kola Penisula, Russia. Boreas, 47 - 56.

Solem T. & Solem J.O. 1997. Shoreline displacement on the coast of Sör-Tröndelag and Möre og Romsdal, Central Norway; a botanical and zoological approach. Norsk Geologisk Tidskrift 77, 193 - 203.

Stabell B. 1980. Holocene shorelevel displacement in Telemark, southern Norway. Norsk Geoglogisk Tidskrift 60, 71 - 81.

Suutarinen O. 1983. Recomputation of land uplift values in Finland. Reports of the Finnish Geodetic Institute 83:1, 1-16.

Svedhage K. 1985. Shore displacement during Late Weichselian and Early Holocene in the Risveden area, SW Sweden. Göteborgs universitet. Geologiska institutionen A 51, 1 - 111.

Sveian H. & Olsen L. 1984. En strandforsyvningskurve fra Verdalsöra, Nord-Tröndelag.Norsk Geologisk Tidskrift 64, 27 - 38.

Svendsen J. I. & Mangerud J. 1990. Sea-level changes and pollen stratigraphy on the outer coast of Sunnmöre, western Norway. Norsk Geologisk Tidskrift 70, 111 - 134.

Svensson N. -O. 1989. Late Weichselian and Early Holocene shore displacement in the Central Baltic, based on stratigraphical and morphological records from Eastern Småland and Gotland, Sweden. Lund University, Department of Quaternary Geology 25, 1 - 195.

Sörensen R. 1979. Late Weichselian deglaciation in the Oslofjord area, south Norway. Boreas 8, 241 - 246.

Thomsen H. 1982. Late Weichselian shore-level displacement on Nord-Jären, south-west Norway. Geologiska Föreningens i Stockholm Förhandlingar 103, 447 - 468.

Walcott R.I. 1970. Isostatic response to loading of the crust in Canada. Canadian Journal of Earth Sciences, 716 - 727.

Winn K., Averdieck F. R., Erlenkeusser H. & Werner F. 1986. Holocene sea level rise in western Baltic and the question of isostatic subsidence. Meyniana 38, 61-80

Vorren K. -D. & Moe D. 1986. The early Holocene climate and sea-level changes in Lofoten and Vesterålen, North Norway. Norsk Geologisk Tidskrift 66, 135 - 143.

Vorren T., Vorren K. -D., Alm T., Gulliksen S., and Lövlie R. 1988. The last deglaciation (20,000 to 11,000 B.P.) on Andöya, northern Norway. Boreas 17, 41-77.

Ziegler P.A. 1990. Geological Atlas of Western Europe. Shell International and Geological Society, London, 2nd ed., 1 - 239.

List of SKB reports

Annual Reports

1977-78
TR 121
KBS Technical Reports 1 – 120
Summaries
Stockholm, May 1979

1979
TR 79-28
The KBS Annual Report 1979
KBS Technical Reports 79-01 – 79-27
Summaries
Stockholm, March 1980

1980
TR 80-26
The KBS Annual Report 1980
KBS Technical Reports 80-01 – 80-25
Summaries
Stockholm, March 1981

1981
TR 81-17
The KBS Annual Report 1981
KBS Technical Reports 81-01 – 81-16
Summaries
Stockholm, April 1982

1982
TR 82-28
The KBS Annual Report 1982
KBS Technical Reports 82-01 – 82-27
Summaries
Stockholm, July 1983

1983
TR 83-77
The KBS Annual Report 1983
KBS Technical Reports 83-01 – 83-76
Summaries
Stockholm, June 1984

1984
TR 85-01
Annual Research and Development Report 1984
Including Summaries of Technical Reports Issued during 1984. (Technical Reports 84-01 – 84-19)
Stockholm, June 1985

1985
TR 85-20
Annual Research and Development Report 1985
Including Summaries of Technical Reports Issued during 1985. (Technical Reports 85-01 – 85-19)
Stockholm, May 1986

1986
TR 86-31
SKB Annual Report 1986
Including Summaries of Technical Reports Issued during 1986
Stockholm, May 1987

1987
TR 87-33
SKB Annual Report 1987
Including Summaries of Technical Reports Issued during 1987
Stockholm, May 1988

1988
TR 88-32
SKB Annual Report 1988
Including Summaries of Technical Reports Issued during 1988
Stockholm, May 1989

1989
TR 89-40
SKB Annual Report 1989
Including Summaries of Technical Reports Issued during 1989
Stockholm, May 1990

1990
TR 90-46
SKB Annual Report 1990
Including Summaries of Technical Reports Issued during 1990
Stockholm, May 1991

1991
TR 91-64
SKB Annual Report 1991
Including Summaries of Technical Reports Issued during 1991
Stockholm, April 1992

1992
TR 92-46
SKB Annual Report 1992
Including Summaries of Technical Reports Issued during 1992
Stockholm, May 1993

1993
TR 93-34
SKB Annual Report 1993
Including Summaries of Technical Reports Issued during 1993
Stockholm, May 1994

1994
TR 94-33
SKB Annual Report 1994
Including Summaries of Technical Reports Issued during 1994
Stockholm, May 1995

1995
TR 95-37
SKB Annual Report 1995
Including Summaries of Technical Reports Issued during 1995
Stockholm, May 1996

1996
TR 96-25
SKB Annual Report 1996
Including Summaries of Technical Reports Issued during 1996
Stockholm, May 1997

List of SKB Technical Reports 1997

TR 97-01
Retention mechanisms and the flow wetted surface – implications for safety analysis
Mark Elert
Kemakta Konsult AB
February 1997

TR 97-02
Äspö HRL – Geoscientific evaluation 1997/1. Overview of site characterization 1986–1995
Roy Stanfors[1], Mikael Erlström[2], Ingemar Markström[3]
[1] RS Consulting, Lund
[2] SGU, Lund
[3] Sydkraft Konsult, Malmö
March 1997

TR 97-03
Äspö HRL – Geoscientific evaluation 1997/2. Results from pre-investigations and detailed site characterization. Summary report
Ingvar Rhén (ed.)[1], Göran Bäckblom (ed.)[2], Gunnar Gustafson[3], Roy Stanfors[4], Peter Wikberg[2]
[1] VBB Viak, Göteborg
[2] SKB, Stockholm
[3] VBB Viak/CTH, Göteborg
[4] RS Consulting, Lund
May 1997

TR 97-04
Äspö HRL – Geoscientific evaluation 1997/3. Results from pre-investigations and detailed site characterization. Comparison of predictions and observations. Geology and mechanical stability
Roy Stanfors[1], Pär Olsson[2], Håkan Stille[3]
[1] RS Consulting, Lund
[2] Skanska, Stockholm
[3] KTH, Stockholm
May 1997

TR 97-05
Äspö HRL – Geoscientific evaluation 1997/4. Results from pre-investigations and detailed site characterization. Comparison of predictions and observations. Hydrogeology, groundwater chemistry and transport of solutes
Ingvar Rhén[1], Gunnar Gustafson[2], Peter Wikberg[3]
[1] VBB Viak, Göteborg
[2] VBB Viak/CTH, Göteborg
[3] SKB, Stockholm
June 1997

TR 97-06
Äspö HRL – Geoscientific evaluation 1997/5. Models based on site characterization 1986–1995
Ingvar Rhén (ed.)[1], Gunnar Gustafson[2], Roy Stanfors[3], Peter Wikberg[4]
[1] VBB Viak, Göteborg
[2] VBB Viak/CTH, Göteborg
[3] RS Consulting, Lund
[4] SKB, Stockholm
October 1997

TR 97-07
A methodology to estimate earthquake effects on fractures intersecting canister holes
Paul La Pointe, Peter Wallmann, Andrew Thomas, Sven Follin
Golder Associates Inc.
March 1997

TR 97-08
Äspö Hard Rock Laboratory Annual Report 1996
SKB
April 1997

TR 97-09
A regional analysis of groundwater flow and salinity distribution in the Äspö area
Urban Svensson
Computer-aided Fluid Engineering AB
May 1997

TR 97-10
On the flow of groundwater in closed tunnels. Generic hydrogeological modelling of nuclear waste repository, SFL 3–5
Johan G Holmén
Uppsala University/Golder Associates AB
June 1997

TR 97-11
Analysis of radioactive corrosion test specimens by means of ICP-MS. Comparison with earlier methods
R S Forsyth
Forsyth Consulting
July 1997

TR 97-12
Diffusion and sorption properties of radionuclides in compacted bentonite
Ji-Wei Yu, Ivars Neretnieks
Dept. of Chemical Engineering and Technology, Chemical Engineering, Royal Institute of Technology, Stockholm, Sweden
July 1997

TR 97-13
Spent nuclear fuel – how dangerous is it? A report from the project "Description of risk"
Allan Hedin
Swedish Nuclear Fuel and Waste Management Co,
Stockholm, Sweden
March 1997

TR 97-14
Water exchange estimates derived from forcing for the hydraulically coupled basins surrounding Äspö island and adjacent coastal water
Anders Engqvist
A & I Engqvist Konsult HB, Vaxholm, Sweden
August 1997

TR 97-15
Dissolution studies of synthetic soddyite and uranophane
Ignasi Casas[1], Isabel Pérez[1], Elena Torrero[1], Jordi Bruno[2], Esther Cera[2], Lara Duro[2]
[1] Dept. of Chemical Engineering, UPC
[2] QuantiSci SL
September 1997

TR 97-16
Groundwater flow through a natural fracture. Flow experiments and numerical modelling
Erik Larsson
Dept. of Geology, Chalmers University of Technology, Göteborg, Sweden
September 1997

TR 97-17
A site scale analysis of groundwater flow and salinity distribution in the Äspö area
Urban Svensson
Computer-aided Fluid Engineering AB
October 1997

TR 97-18
Release of segregated nuclides from spent fuel
L H Johnson, J C Tait
AECL, Whiteshell Laboratories, Pinawa, Manitoba, Canada
October 1997

TR 97-19
Assessment of a spent fuel disposal canister. Assessment studies for a copper canister with cast steel inner component
Alex E Bond, Andrew R Hoch, Gareth D Jones, Aleks J Tomczyk, Richard M Wiggin, William J Worraker
AEA Technology, Harwell, UK
May 1997

TR 97-20
Diffusion data in granite Recommended values
Yvonne Ohlsson, Ivars Neretnieks
Department of Chemical Engineering and Technology, Chemical Engineering, Royal Institute of Technology, Stockholm, Sweden
October 1997

TR 97-21
Investigation of the large scale regional hydrogeological situation at Ceberg
Anders Boghammar[1], Bertil Grundfelt[1], Lee Hartley[2]
[1] Kemakta Konsult AB, Sweden
[2] AEA Technology, UK
November 1997

TR 97-22
Investigations of subterranean microorganisms and their importance for performance assessment of radioactive waste disposal. Results and conclusions achieved during the period 1995 to 1997
Karsten Pedersen
Göteborg University, Institute of Cell and Molecular Biology, Dept. of General and Marine Microbiology, Göteborg, Sweden
November 1997

TR 97-23
Summary of hydrogeologic conditions at Aberg, Beberg and Ceberg
Douglas Walker[1], Ingvar Rhén[2], Ioana Gurban[1]
[1] INTERA KB
[2] VBB Viak
October 1997

TR 97-24
Characterization of the excavation disturbance caused by boring of the experimental full scale deposition holes in the Research Tunnel at Olkiluoto
Jorma Autio
Saanio & Riekkola Oy, Helsinki, Finland
September 1997

TR 97-25
The SKB Spent Fuel Corrosion Programme.
An evaluation of results from the experimental programme performed in the Studsvik Hot Cell Laboratory
Roy Forsyth
Forsyth Consulting
December 1997

TR 97-26
Thermoelastic stress due to a rectangular heat source in a semi-infinite medium. Application for the KBS-3 repository
Thomas Probert, Johan Claesson
Depts. of Mathematical Physics and Building Physics, Lund University, Sweden
April 1997

TR 97-27
Temperature field due to time-dependent heat sources in a large rectangular grid. Application for the KBS-3 repository
Thomas Probert, Johan Claesson
Depts. of Mathematical Physics and Building Physics, Lund University, Sweden
April 1997

ISSN 0284-3757
CM Gruppen AB, Bromma, 1998